CONCEPTUAL GEOCHEMICAL MODEL FOR THE ALLUVIAL AQUIFER

Grants Reclamation Project

Homestake Mining Company
Cibola County, New Mexico
September, 2020

Prepared For:
Homestake Mining Company
P.O. Box 98, Highway 605
Grants, NM 87020

Prepared By:
Worthington Miller Environmental, LLC
1027 W. Horsetooth Rd., Ste. 200
Fort Collins, Colorado 80526

TABLE OF CONTENTS

LIST OF TABLES

LIST OF FIGURES

EXECUTIVE SUMMARY

This report presents the first comprehensive conceptual geochemical model (CGM) developed for the Homestake Mining Company (HMC) Grants Reclamation Project in Cibola County, New Mexico. The CGM represents a conceptualization of Large Tailings Pile (LTP) contaminant sources and transport through the underlying San Mateo Creek (SMC) Alluvial Aquifer system. The LTP received U mill tailings generated from processing of sandstone-hosted U ore mined from the Grants Uranium District using an alkaline recovery process. The mill effluent was a moderately-oxidizing, alkaline, Na-SO_4 type water with elevated concentrations of U, Mo, Se, and indicator parameters (Cl, SO_4). The LTP encompasses approximately 200 acres containing 22 million tons of tailings and has been partially reclaimed. Historic tailings seepage has produced elongated U contaminant plumes in the direction of flow to the west and south in the SMC alluvium. The active source is contained within a dissipating mound of tailings water in the LTP which seeps into the underlying Alluvial Aquifer. Redox conditions in the tailings range from oxic to suboxic, with the primary COCs occurring as $UO_2(CO_3)_3^{4-}$, MoO_4^{2-}, and SeO_3^{2-} (selenite) which tend to remain soluble. Tailings seepage which migrates into the Alluvial Aquifer becomes partially diluted as it mixes with more oxidizing Ca-SO_4 type water from upgradient. As the tailings-influenced groundwater moves downgradient, the conservative indicator constituents (Cl, SO_4) are controlled by dilution and dispersion. Uranium speciation becomes dominated by $CaUO_2(CO_3)_3^{2-}$, selenate (SeO_4^{2-}) becomes the main form of Se, and Mo remains as the molybdate ion (MoO_4^{2-}). A residual source term contains those solid-phase forms of COCs with the potential for release into infiltrating water following tailings drain down. This includes pyrite, elemental Se, MoS_2, and various forms of U. Static testing has shown the tailings have excess acid neutralizing capacity and are non-acid generating. Kinetic tests results indicate no significant release of Fe, SO_4, acidity, or COCs upon accelerated weathering, such that their long-term concentrations are not expected to significantly increase in the infiltrating water. Due to the onset of reducing conditions within and beneath the LTP, Se concentrations have been decreasing over time.

In the immediate vicinity of the LTP, mixing of tailings seepage with Ca-SO_4 groundwater and reaction with calcite in the alluvium promotes precipitation of powellite ($CaMoO_4$) which limits the concentration of Mo to between 0.1 and 1 mg/L outside of the LTP. With increasing distance from the LTP, the COCs are partially attenuated by ferrihydrite adsorption to varying degrees, depending on factors such as pH, alkalinity, Eh, TDS, and concentrations of competing adsorbing species. Some areas of the groundwater may be slightly reducing, such that selenate may be reduced to selenite or perhaps precipitate as elemental Se. The fraction of COCs which remain in solution continue to migrate downgradient and are eventually attenuated to concentrations below Site standards through additional groundwater mixing, dilution, and limited adsorption to mineral surfaces. The CGM presented here provides a basis for ongoing development of computational geochemical models to predict post-closure transport of COCs in the SMC Alluvial Aquifer.

1.0 INTRODUCTION

Homestake Mining Company (HMC) has managed a groundwater restoration program since 1977 at the Grants Reclamation Project Site (Site) in Cibola County, New Mexico (Figure 1), with the goal of reducing concentrations of constituents of concern (COCs) in underlying aquifers to meet Site standards. Uranium (U) milling operations resulted in the placement of tailings into the small tailings pile (STP) and the large tailings pile (LTP). The STP is an unlined impoundment covering about 40 acres that was used to contain approximately 2 million tons of tailings from ore milled under contracts with the federal government (1958 to 1962). The LTP is an unlined impoundment covering about 200 acres and contains approximately 22 million tons of tailings from ore processed under both federal and commercial contracts (1958 to 1990). The tailings pore water contains elevated levels of COCs which included U, selenium (Se), molybdenum (Mo), sulfate (SO_4), chloride (Cl), total dissolved solids (TDS), nitrate-nitrogen (NO_3-N), vanadium (V), thorium-230 (Th-230), and radium-226+228 (Ra-226+228). Although the tailings have been partially reclaimed, a defined contaminant plume still exists in the alluvial aquifer. However, source and plume control have since proven effective in reducing the concentrations of COCs in tailings and the extent of impacted groundwater.

Localized groundwater contamination of the San Mateo alluvial aquifer was first observed and reported in 1961 (Chavez, 1961). An alluvial contaminant plume was later identified in 1976 originating from the LTP and moving off-Site to the south and west. Consequently, a series of injection wells were installed along the southern Site boundary in 1977, creating a hydraulic barrier to inhibit contaminant migration across the Site boundary. A complementary series of groundwater extraction wells was also installed in the vicinity of the tailings piles between 1977 and 1982 to collect tailings seepage. Following mill closure in 1990, the hydraulic barrier system was incorporated into the Site groundwater restoration program. Toe drains were also installed at the perimeter of the LTP in 1992 to collect tailings seepage. A reverse osmosis (RO) plant was constructed in 1999 to assist with Site water management, which has periodically been used to treat water for injection into the alluvial aquifer, followed by initiation of tailings flushing and land application in 2000. Three evaporation ponds were also constructed between 1990 and 2010 to assist with overall water management.

The resulting Corrective Action Program (CAP) for the Site encompassed five operational components: (1) source control through tailings flushing to expedite LTP seepage drain down to groundwater, (2) plume control by creation of a hydraulic barrier, (3) RO treatment to remove COCs from groundwater and to supply additional clean water for re-injection, (4) evaporation, and (5) land treatment. Source control began in 1995 when HMC initiated a tailings dewatering program in the LTP to remove tailings pore water. The full-scale implementation of the tailings flushing program began in 2002 and was terminated in 2015.

HMC is working toward Site closure with concurrent development of Site-wide hydrologic and geochemical models to evaluate post-closure fate and transport of COCs. Both regional and Site-wide hydrologic conceptual models were recently developed for the Site (Brown and Caldwell, 2018), although a comprehensive Site conceptual geochemical model (CGM) has not been previously developed. In 2018, HMC began collecting detailed geochemical information regarding chemical and mineralogical tailings characteristics, aquifer properties, and oxidation-reduction (redox) conditions in the LTP and alluvial groundwater. A Site-wide CGM was subsequently produced, which in turn has

provided the basis for ongoing development of robust computational geochemical models to predict post-closure fate and transport of COCs. This report presents the current CGM based on a summary of existing data and the geochemical data collected from 2018 through 2020 (WME, 2020a,b).

2.0 MILL OPERATIONAL HISTORY

HMC and its affiliates recovered U from 1958 through 1990 at a location which is now the Grants Reclamation Project (Figure 1). The Site contained two mills (McLemore, 2007): (1) a southern mill known as the Homestake-New Mexico Partners mill, built in 1957 and closed in 1962, and (2) a larger mill located north of the original facility, built in 1957 by the Homestake-Sapin Partners, a partnership between Homestake Corporation and Sabre Pinon Corporation. Uranium production began in 1958 with an initial ore processing capacity of 1,750 tons per day (tpd). Mill modifications increased the total processing capacity to 3,400 tpd by the early 1960's. In 1962, the United Nuclear Corporation merged with Sabre Pinon Corporation but maintained the United Nuclear Corporation name. United Nuclear Corporation became the limited partner with Homestake, forming the United Nuclear-Homestake Partnership (UN-HP). In March 1981, the UN-HP partnership was disbanded and Homestake became the sole owner. Uranium production ceased at the Site in 1981, but the mill reopened in 1988 to process local ore until mill closure in 1990.

The Homestake mill and associated structures were decommissioned and demolished between 1993 and 1995, with debris being buried on-Site in eight pits. Five of the eight pits were located in the mill area between the LTP and State Highway 605, and the remaining three pits were located between the LTP and Evaporation Pond (EP) -1 and -2. Demolition debris primarily consisted of metal and wood from buildings, milling equipment, and concrete foundations. Pits were typically 20 ft deep and debris was placed into the pits in 5-ft lifts. After each lift was in place, grout was pumped into the pit to fill voids around the debris and to solidify the debris to prevent contact with the environment. Once filled, a soil cover was place over the pits and surrounding areas and graded for positive drainage. The soil cover was approximately 2 ft thick over the mill area and 4 to 5 ft thick over some of the pits. An earth levee was constructed north of the former mill to divert runoff from the area.

3.0 ORE SOURCE AND CHARACTERISTICS

The mineralogy of the ore and the leaching process used to extract U are primary factors controlling the chemical characteristics of U mill tailings. Uranium ore processed at the Homestake mill was sourced from various mines located in the Grants Uranium District (District), which consisted of eight subdistricts extending from east of Laguna to west of Gallup in the San Juan Basin of northwestern New Mexico. Between 1951 and 1980, the District produced more U than any other area in the United States (McLemore, 2007). The most important type of deposit in terms of production and resources in this region are the sandstone-hosted U deposits in the Westwater Canyon Member of the Morrison Formation, consisting of either: (1) primary (trend or tabular) deposits, (2) redistributed (roll-type) deposits, or (3) remnant deposits (Figures 2 and 3). Uranium deposits within the Todilto Limestone have also played an important role in historical production within the District. Uranium in these deposits originated from leaching of either altered volcanic ash or granitic rocks, and was subsequently transported by ground and surface waters into the Todilto Limestone and Morrison Formation, where the presence of organic material facilitated precipitation of U.

Localization of U in sandstone deposits is most often attributed to reduction and precipitation of soluble U(VI) (Figure 3). Reducing agents include pyrite (FeS_2), hydrogen sulfide (H_2S), and organic matter. Uranium mineralization in sandstone deposits is commonly associated with detrital organic matter, where reduced U(IV) minerals such as uraninite (UO_2) and coffinite [$U(SiO_4)_{1-x}(OH)_{4x}$] occur within the organic fragments and interstitially within the sandstone. Pyrite is invariably present and also found in association with organic matter and disseminated throughout the sandstone. Enrichment of associated elements such as Mo, Se, and V is also common in sandstone-type U deposits (Nash et al., 1981). Minor amounts of sulfides (primarily pyrite and marcasite) with significant amounts of elemental Se and Mo sulfide (MoS_2) are characteristic of sandstone ore in the District (Rosenzweig, 1961). Selenium may also occur as iron (Fe) selenide ($FeSe_2$) or may substitute for sulfur (S) in pyrite up to 3% by weight (Coleman and Delevaux, 1957). Vanadium may occur as V(III) minerals (V-mica, roscoelite) and V(IV) minerals (mica-montmorillonite). Weathered and oxidized facies of sandstone-type deposits commonly retain their original grade because the oxidized U and V tend to combine as tyuyamunite [$Ca(UO_2)(VO_4)_2 \cdot (5\text{-}8)H_2O$] and carnotite [$K_2(UO_2)_2(VO_4)_2 \cdot 3H_2O$] (Nash et al., 1981), which are abundant in all ore types within the District (Rosenzweig, 1961).

Limestone is not typically considered a favorable host rock for U mineralization due to its inherent low permeability and paucity of organic material and other reducing agents. However, more than 100 mines and occurrences are found in the Todilto Limestone in New Mexico, and approximately 2% of the U production from the San Juan Basin from 1947 to 2002 was from the Todilto Limestone. The organic-rich limestones were locally deformed by the overlying Summerville or Wanakah Formations producing intraformational folds in the Todilto Limestone. Uraniferous waters carrying dissolved U(VI) migrated into the folds and associated fractures where the U precipitated in the presence of organic matter (McLemore, 2007). Thus, the ore is generally of the unoxidized type, although fracture zones are commonly coated with oxidized U and V minerals (Rosenzweig, 1961).

4.0 ORE PROCESSING

The primary source of ore for the Homestake mill was from underground mines located within 30 miles of the Site in the Ambrosia Lake subdistrict. Two basic types of U ore were known to have been processed by the mill: (1) sandstone ore (80 to 85% of the mill feed) and (2) limestone ore (15 to 20% of the mill feed) (Skiff and Turner, 1981). Uranium mineralization occurred as coffinite, uraninite, tyuyamunite, and carnotite as impregnations, pore fillings, and cementation between sand grains. The ore grade ranged from 0.04 to 0.3% as U_3O_8. Uranium mineralization was associated with carbonaceous material and contained lesser amounts of Mo and Se.

Milling of the ore was conducted in five general stages: (1) ore handling/preparation, (2) extraction, (3) liquid-solid separation, (4) precipitation/purification, and (5) product preparation (Skiff and Turner, 1981). The recovery process utilized two parallel circuits for ball-milling, thickening, and leaching of the ore: the North Circuit was used to process the majority of sandstone ore, while the South Circuit used a secondary grind and longer leach time to process the refractory limestone ore. An alkaline leaching process was used to extract U from the thickened slurry. Chemical reagents utilized included sodium carbonate (Na_2CO_3, 37 g/L), sodium bicarbonate ($NaHCO_3$, 7 g/L), polyacrylamide flocculant, sodium hydroxide (NaOH), sulfuric acid (H_2SO_4), and ammonia (NH_3) (Skiff and Turner, 1981). Alkaline extraction is based on the enhanced dissolution of U minerals by

dissolved carbonate, producing stable U(VI) tricarbonate solution species [$UO_2(CO_3)_3^{4-}$(aq)] (Butler, 1972; Skiff and Turner, 1981). When U is present as UO_2, effective dissolution through carbonate complexation requires that tetravalent U(IV) first be oxidized to hexavalent U(VI):

$$UO_2(s) + 0.5O_2(g) \rightarrow UO_3(s) \quad [1]$$

All of the oxidized U then dissolves in the presence of carbonate to form soluble U(VI) tricarbonate:

$$UO_3(s) + 3Na_2CO_3(s) + H_2O(l) \rightarrow [UO_2(CO_3)_3]^{4-}(aq) + 6Na^+(aq) + 2OH^-(aq) \quad [2]$$

In order to achieve maximum U solubility, excess Na_2CO_3 was added to neutralize hydroxide (OH^-) produced in Equation [2]. The thickened slurry was leached in a two-stage circuit, where the first stage consisted of a high pressure and temperature leach (414 kPa at 93°C) for 4.5 hr. The second stage utilized a 12-hr atmospheric pressure leach at 77°C for the sandstone ore and 24 hr. for the limestone ore. Leached slurries were then processed through three levels of filtration: (1) first stage filtrate containing the pregnant U solution was sent to the clarifier before the precipitation circuit, (2) second stage filtrate was sent to the mill solution circuit, and (3) third stage filtrate was used as a wash and repulper solution on the first stage of filters. Filter cake from the third stage was repulped with recycled tailings pond solution and slurried for tailings disposal (Skiff and Turner, 1981).

Pregnant solution from the clarifier was then pumped to the precipitation circuit after heating to 82°C and precipitation was conducted in two stages. First, pregnant solution was mixed with recycled sodium diuranate (yellow cake) to increase the soluble U content. Second, NaOH was added to obtain a pH >12 and precipitate the U as sodium diuranate (Butler, 1972; Skiff and Turner, 1981):

$$2[UO_2(CO_3)_3]^{4-}(aq) + 6OH^-(aq) + 2Na^+(aq) \rightarrow Na_2U_2O_7(s) + 6CO_3^{2-}(aq) + 3H_2O(l) \quad [3]$$

The precipitate contained approximately 5 to 77% U_3O_8 and 5 to 6% V_2O_5 with excess Na_2CO_3, and consequently the yellow cake required purification prior to market release. Purification to remove excess V and sodium (Na) involved the use of H_2SO_4 to dissolve the yellow cake slurry, NH_3 for pH adjustment, and ammonium sulfate [$(NH_4)_2SO_4$] for washing the reprecipitated yellow cake. The product was then pumped to a dryer to remove excess water and residual NH_3, and the yellow cake was packaged into 55-gallon drums which were sealed, weighed, and cleaned prior to shipment.

5.0 MILL TAILINGS DISPOSAL AND CHARACTERISTICS

Milling operations produced the two tailings piles (STP and LTP) which currently exist at the Site. The STP operated from 1958 to 1962 and contains tailings generated exclusively from ore milled under U.S. Atomic Energy Commission (AEC) contracts. Tailings placed into the STP were contained by a native soil embankment which was compacted using heavy equipment and brought to a height of 20 to 25 ft. The crest was a minimum of 10 ft wide with an approximate 40 ft wide base. Pond EP-1 was constructed on the north area of the STP in 1990 to assist with LTP water management and is also used for evaporation of collection well water and RO brine from the water treatment plant.

The LTP was operated from 1958 through 1990, and covers approximately 234 acres with a height ranging from 70 to 90 ft. The LTP contains approximately 11.4 million tons of tailings produced under AEC contracts, and 10.9 million tons of tailings produced from commercial contracts, for a total of about 22 million tons (Figure 4). Except for a small starter dike, the LTP was constructed of hydraulically-placed tailings that were initially deposited into the East Cell of the LTP in 1958, until

the West Cell was added in 1966. The starter dike utilized native soils from the immediate area and was constructed in compacted 6-in lifts, to a height of approximately 10 ft, with a width of 10 to 15 ft at the crest and 25 to 30 ft at the base. The perimeter dike was raised using the centerline method until 1981, when an inboard offset of the embankment was made to improve stability. Subsequent lifts were added to the offset perimeter dike using the centerline method.

Filter cake from the liquid-solid separation mill circuit was repulped with recycle solution from the tailings pond ion exchange system and transported to a tailings slurry tank (Skiff and Turner, 1981). The LTP was constructed by pumping the tailings slurry (40% solids) through 20-in cyclones. The coarser sands were deposited downstream of the dike crest along the centerline to raise the pile, while the finer materials (slimes) were deposited upstream of the dike crest toward the pond center of each cell. The tailings liquid was recovered through two decant towers for reuse as mill process water. In the latter stages of mill operations when production rates were low, cyclone separation was discontinued and the tailings slurry was discharged directly across the beaches. Tailings disposal was then confined to a single pond at a time, with the other pond being used for evaporation as needed.

5.1 Physical Tailings Characteristics

A field and laboratory investigation was conducted in 1980 to evaluate the long-term stability of the LTP embankments and to assess compliance with the State of New Mexico Criteria for Uranium Mills (D'Appolonia, 1980). The field program consisted of 14 borings and installation of 20 piezometers. The borings were advanced to provide samples of tailings and native soils for strength, permeability, and classification testing. Additional stratigraphic details were obtained from the borings and combined with the results of a previous investigation (IECO, 1977). The borings also provided access for installing piezometers to measure water levels in the tailings embankment and the native soils.

The LTP embankment was primarily constructed using sands, while the slimes were deposited in the East and West ponds. However, analysis of materials from LTP borings indicated a mixture of materials, ranging from predominantly fine to predominantly coarse. The intermixture results from sedimentation of progressively finer materials away from the cyclone which was moved along the crest of the embankment, creating successive overlapping deltas (D'Appolonia, 1980). Areas near the tailings embankment primarily received the coarser tailings particles which settled from suspension more rapidly than the finer silts which were transported to the center of the pond. Thus, no distinct interface exists between the coarse and fine tailings; rather areas behind the tailings embankment are characterized as being inter-fingered zones of coarse and fine tailings with occasional silty lenses, where the percentage of silty material increases away from the embankment centerline.

Laboratory testing (D'Appolonia, 1980) showed the tailings are largely composed of silt to fine-sand sized particles. The sands contained 5 to 12% silt by weight, while the slimes contain 15 to 30% silt by weight. Grain size analysis of 22 tailings samples showed 90% of the material passed through a No. 40 sieve and 5 to 20% passed a No. 200 sieve, with little spatial grain-size variation among locations. The average moisture content was 8.3% in unsaturated coarse tailings and 23.8% in saturated coarse tailings. Fines were only encountered in two borings with an average moisture content of 25%. Measured densities in the embankment vicinity ranged from 78.4 to 115.5 lbs./ft^3 (1.25 to 1.85 g/cm^3), with an average density of 96 lbs./ft^3 (1.5 g/cm^3). The corresponding calculated porosities range from approximately 53 to 30%, with an average of 43%. The average permeability

of the tailings was 10^{-4} cm/sec, while that of the underlying alluvium was 5 x 10^{-5} cm/sec. In a subsequent investigation, GEOCHEM (1992) analyzed 30 samples of sands and slimes from the LTP and reported clay contents (<2 μm) ranging from 14 to 50% in slimes and 5 to 14% in sands.

Due to the lower conductivity of the underlying alluvium, a saturated zone formed within the LTP above the ground surface during operations. The phreatic surface within the tailings sloped toward the edge of the LTP, producing seepage on the side slopes. Piezometric water levels in 1980 showed a thinner saturated thickness and lower seepage face in the West Cell compared to the East Cell, likely due to a low pond level and lack of recent disposal activity. Seepage flowed laterally and vertically at rates determined by physical properties of the tailings and alluvium (Figure 5). Due to confining effects of the underlying alluvium, downward flow was considered negligible compared to the horizontal flow potential. These conditions produced apparent seepage emanation above phreatic levels at the toe of the impoundment, which was assumed to result from capillary rise. In 1980 it was noted that unsaturated seepage of tailings fluid below the LTP had produced a groundwater mound in a perched zone of the alluvium, where the elevation of the mound beneath the embankment crest was generally about 20 ft higher than the phreatic surface at the toe of the LTP (D'Appolonia, 1980).

5.2 Chemical and Mineralogical Tailings Characteristics

Uranium mill tailings contain elevated trace element concentrations due to natural enrichment processes during ore formation. As a result, their concentrations in mill tailings may be a factor of 5 to 100 times higher compared to local background soils (NAS, 1986). Reported enrichment factors from Colorado Plateau Morrison Formation ore are: U = 830, V = 575, Mo = 65, and Se = 45 (Thamm et al., 1980). Sandstone ore from the Grants Mineral Belt can contain: 0.10% to 1.3% U_3O_8 (mean = 0.16%), 30 to 15,000 ppm V (mean = 634 ppm), 0.3 to 15,000 ppm Mo (mean = 22 ppm), and 0.4 to 11,000 ppm Se (mean = 60 ppm) (mean = 38 ppm) (NAS, 1986; McLemore, 2007). The sources of these constituents in mill tailings originate from their occurrence in ore as U oxides, silicates and/or vanadates, native Se or ferroselite ($FeSe_2$), V oxides or roscoelite, and Mo sulfide (Section 3).

The chemical and mineralogical properties of U mill tailings are thus controlled by both ore characteristics and the type of milling process (acid or alkaline) employed. Morrison Formation sandstones contain an abundance of detrital minerals such as quartz (85%), feldspar (8%), and silicified tuff and chert (7%) with the remaining mass consisting of carbonate cement (15%), volcanic fragments (4%), and minor minerals (magnetite, ilmenite, mica) (Thamm et al., 1980). The presence of silicified and carbonized wood is also very common. Uranium mill tailings contain more than 99% of the mass of the original ore (NAS, 1986). Consequently, the coarse tailings fractions are chiefly composed of primary minerals that have resisted the leaching process (quartz, feldspars). The fines consist mainly of clays, gypsum, barite, plus Fe, Al, and manganese (Mn) oxides (Abdelouas, 2006).

While conventional mills extract 90 to 95% of U from the ore, about 85% of the radioactivity from the original ore remains in the tailings (Landa, 1980). The components of the U-238 decay series with the longest half-lives, and consequently of most environmental concern, are U-238, U-234, Th-230, Ra-226, and Pb-210. The U and accompanying trace elements which remain in the mill tailings may be associated with clays, organic matter, Fe and Al oxides, or may still exist in their original mineralogic form. Because naturally-occurring U contains 99.3% (by weight) U-238, and Th-232 contents are low in U ore mined in the United States, the bulk of radioactivity in tailings is associated

with the U-238 decay series. In the LTP, fine tailings contain a higher concentration of radioactive elements compared to coarser tailings (fine to coarse): Ra-226 (630 to 65 pCi/g), Th-230 (0.081 to 0.0116 pCi/g), Pb-210 (840 to 99 pCi/g), and U_3O_8 (0.011 to 0.004%) (HMC, 1982).

5.3 Historic Tailings Water Quality

Mill tailings solutions produced from alkaline leaching of U ore in the Grants Mineral Belt are known to contain elevated pH and dissolved concentrations of Na, SO_4, NO_3-N, TDS, trace elements, and radionuclides (USEPA, 1975). Early chemical analyses of LTP tailings solution conducted between 1978 and 1981 (HE, 1983) and from an LTP sump between 1977 and 1979 (NMHED, 1980) are presented in Table 1. The solution was alkaline (pH ≥ 9.9) with elevated TDS, and dominated by Na, SO_4, Cl, and bicarbonate (HCO_3) from the use $NaHCO_3$, Na_2CO_3, and H_2SO_4 during milling. The average concentrations of U, Se, and Mo in the tailings solution were 36.8 mg/L, 25.4 mg/L, and 88.6 mg/L, respectively, and were in good agreement with the average values for the sump (Table 1). The mean U concentration of 150 mg/L reported by USEPA (1975) was notably higher compared to the remaining values, whereas the average Se was lower compared to the subsequent analyses. Aluminum (Al), barium (Ba), cadmium (Cd), lead (Pb), and zinc (Zn) were low or below detection in the tailings water. Oxidation of NH_3 used in milling produced moderate levels of NO_3-N. The solution was elevated in Ra-226 and Pb-210 with gross alpha activity up to 10,000 pCi/L.

6.0 TAILINGS RECLAMATION AND SOURCE CONTROL

The STP was partially reclaimed from 1993 to 1995 due to the construction of EP-1 in 1990. An interim cover was completed in May 1997 for the portion of the STP not covered by EP-1. The 12-in compacted interim cover material for the STP was obtained from borrow areas near the LTP. Windblown materials were removed from the surrounding area and placed on the tailings pile before covering. An average 1-ft depth of soil was placed on top of the STP as an interim cover and is awaiting final settlement before the final radon (Rn) barrier is placed on top of the current cover. The STP contains no saturation and is no longer a significant source of COCs to groundwater.

The LTP was partially reclaimed between 1993 and 1995 to allow for settlement of the fill material and to accommodate ongoing groundwater restoration. A Rn barrier was placed on the north, west, and south side slopes, followed by placement of an interim cover on top of the LTP in the fall of 1994. Placement of the Rn barrier on the east side slopes occurred in July 1995. A final erosion protection layer of rock approximately 6- to 9-in thick was placed on the side slopes of the LTP. In December 1996, minor fill replacement and maintenance of the interim cover on the top of the LTP was completed. The top cover consists of an average 1-foot of soil obtained from borrow areas near the LTP. The interim cover is awaiting final settlement before the final Rn barrier and rock cover are placed on top of the current cover.

Groundwater remediation activities have been implemented in parallel with the LTP surface reclamation. Plume control began in 1977 with installation of injection wells and infiltration lines along the southern Site boundary to create a hydraulic barrier preventing downgradient migration of the plume. Additional plume control between 1977 and 1982 included installation of groundwater extraction wells near the tailings and evaporation ponds for seepage collection. Source control was initiated in 1995 when HMC began dewatering operations at the LTP, followed by full-scale implementation of the LTP flushing program in 2002. The flushing program involved injection of

slightly-impacted water into the LTP with subsequent extraction of LTP pore water for treatment or disposal. Approximately 480 million gallons of water were removed between 1995 and 2014, and the flushing program was discontinued in July 2015. Collection and treatment of tailings water has continued, and the calculated mass of contaminants removed from toe drains and tailings through 2019 includes over 2,500 kg of Se, 217,000 kg of Mo, and 91,000 kg of U (HMC and HE, 2020). Source control activities have significantly reduced LTP pore water U concentrations since 2000 (Figure 6).

7.0 ALLUVIAL AQUIFER HYDROGEOLOGY

Four primary geologic units occur at the Site: (1) Quaternary alluvium, (2) Chinle Formation, (3) San Andres Limestone, and (4) Glorieta Sandstone (Brown and Caldwell, 2018). Alluvium underlies the entire Site and is typically 50 to 100 ft thick. The underlying Chinle Formation may be up to 900 ft thick and is comprised of three water-bearing units referred to as the Upper Chinle Sandstone, the Middle Chinle Sandstone, and the Lower Chinle Mudstone. The lowermost units are the San Andres Limestone and Glorieta Sandstone with a combined thickness of 200 to 225 ft. The alluvial aquifer is the primary aquifer of concern because it is the most contaminated and recharges the Chinle Aquifer system which has been used as a drinking water source by local residents (ATSDR, 2009).

The Alluvial Aquifer system is composed of three distinct but connected aquifers: San Mateo Creek (SMC), Rio Lobo, and Rio San Jose (HDR, 2020). The Site sits within the SMC aquifer in the vicinity of where the Rio Lobo tributary feeds in from the east. A local bedrock high located to the southwest causes the SMC groundwater to branch into two flow paths that feed into the Rio San Jose. One branch flows directly west of the LTP to the north of the bedrock high into the Rio San Jose, and the other flows south before trending southwest on the southern edge of the bedrock high (Figure 7). The Alluvial Aquifer is unconfined with saturated thickness ranging from 0 to 70 ft, and depth to groundwater ranging from 40 to 60 ft below ground surface. The SMC and Rio Lobo alluvium have been characterized as very fine to coarse sand with small and discontinuous silt and clay lenses (HDR, 2020). Hydraulic conductivity (K_{sat}) ranges from 10 to more than 200 feet/day (ft/d), with the highest K_{sat} values being measured in a paleochannel located directly west and southwest of the LTP. Alluvial groundwater flow at the Site originates from the northeast in the SMC alluvium. The alluvial groundwater flows beneath the LTP and STP, after which groundwater flow bifurcates around a local bedrock high into two branches (Figure 7): one branch flows west toward the Rio San Jose alluvium, while the other branch flows south through the Rio Lobo alluvium and toward the Rio San Jose alluvium (Brown and Caldwell, 2018).

8.0 EXTENT OF GROUNDWATER IMPACTS

The influence of U mining and milling on surface water quality in the District was recognized by the 1950's, although at that time the effects on groundwater had not yet been investigated (Kaufmann et al., 1976). By the early 1960's however, elevated levels of Ra were detected in alluvial groundwater at the Site (Chavez, 1961). Later studies in the 1970's identified elevated levels of Ra, U, and Se in shallow alluvial groundwater being used for domestic purposes in downgradient subdivisions (USEPA, 1975). In 1976, a defined contaminant plume was identified in the alluvial aquifer originating from the LTP and moving off-Site to the South and West (HMC, 2019). In 1977, UN-HP began operating a line of groundwater injection wells along the southern Site boundary, creating a hydraulic barrier to limit migration of the contaminant plume across the Site boundary. Since 1977,

HMC has progressively improved and expanded the groundwater remediation system, and the combination of injection and collection has significantly withdrawn the contaminant plume.

The Site constituents of most concern are U, Mo, Se, SO_4, Cl, and TDS, and their long-term trends in groundwater have been decreasing due to groundwater restoration activities (HMC, 2019). Prior to implementation of restoration in 1976, Se concentrations exceeding the Site standard of 0.32 mg/L in the Alluvial Aquifer extended about 2,000 ft southwest of the LTP and 1,400 ft southwest of the STP (Figure 8). Selenium was also elevated in the vicinity of the Broadview Acres subdivision. Selenium concentrations in the alluvium below the LTP and at Broadview Acres declined significantly after 1976. By 1999, Se concentrations only exceeded the Site standard below the LTP and STP, in an area extending outward from the tailings up to 800 ft, and in a narrow plume southwest of the Felice Acres subdivision. Selenium concentrations have continued to decline, and areas which currently exceed the Site standard are limited to the immediate vicinity of the LTP and STP (Figure 8).

Uranium later became the most important parameter for restoration after establishment of new standards in the mid-2000's (HMC and HE, 2020). The current Site standard for U in the Alluvial Aquifer is 0.16 mg/L. As early as 1976, U concentrations exceeded 10 mg/L in alluvial groundwater near the LTP/STP and in the western Broadview Acres subdivision (Figure 9). The full extent of the U plume was delineated with additional wells in the 1990's, where two U plumes (South Off-Site and North Off-Site) were identified (HMC, 2019). In 1999, the South Off-Site plume occurred southwest of the Felice Acres subdivision, while the North Off-Site plume extended west of the LTP where it comingled with the Bluewater Disposal Site plume in the Rio San Jose alluvium. The western extent of the North Off-Site plume has since been retracted by approximately 1 mile, and U concentrations have been significantly reduced in the South Off-Site plume as a result of groundwater collection and treatment. The 2018 distribution of U in the alluvial groundwater (Figure 9) shows the extent of elevated concentrations in the vicinity of the LTP/STP and the current extent of the two U plumes.

Migration of Mo in the alluvial aquifer has historically been less extensive compared to U and Se. The current Site standard for Mo in the Alluvial Aquifer is 0.1 mg/L. In 1976, elevated Mo concentrations extended about 1,000 ft west of the LTP and 1,800 ft southwest of the STP, with concentrations exceeding 50 mg/L below the tailings (Figure 10). Molybdenum concentrations >1 mg/L also existed in Broadview Acres. By 1999, the area in Broadview Acres had been restored, but a small plume was present in Felice Acres. The 2018 distribution of Mo in the alluvial groundwater (Figure 10) shows that elevated concentrations primarily occur in the vicinity of the LTP/STP, and to a lesser extent in areas west of the LTP and southeast of the STP.

9.0 TAILINGS AND ALLUVIAL AQUIFER GEOCHEMISTRY

For contaminant transport assessment at U mill tailings sites, geochemical conditions should be sufficiently characterized to: (1) estimate the source term, (2) describe the subsurface geochemical properties, and (3) identify contaminant attenuation mechanisms (USNRC, 2003). In 2018, HMC initiated a 2-year characterization study to assess geochemical conditions within the tailings and the alluvial groundwater system (WME, 2020a,b). The objectives were to characterize the solid-phase geochemistry of tailings and alluvium, together with geochemical conditions in the tailings solution and alluvial groundwater, to better understand the factors controlling transport of U, Mo, and Se.

Detailed water quality analysis of selected existing LTP wells, new short-screen (5 ft) LTP wells, LTP sumps, and alluvial groundwater included: major cations (Ca, Mg, Na, K), anions (Cl, SO_4, alkalinity, F), metals (Fe, Al, Mn, Ba), nutrients (NO_3-N, NH_3-N, P), sulfide (H_2S), dissolved organic carbon (DOC), and U, V, Mo, and Se). Temperature, pH, specific conductivity (SC), dissolved oxygen (DO), and oxidation-reduction potential (ORP) were measured in the field using a flow cell to prevent contact with the atmosphere. Redox conditions were evaluated by assessing DO content, redox potential (expressed as Eh), and redox couples (Fe^{2+}/Fe^{3+}, NH_4^+/NO_3^-, H_2S/SO_4^{2-}).

Samples of the LTP tailings solids and San Mateo Alluvium were characterized for: (1) bulk and clay mineral composition using X-ray diffraction (XRD) and scanning electron microscopy (SEM), (2) static acid-base accounting (ABA) with sulfur forms, and (3) mineral partitioning of U, Se, and Mo using sequential selective extraction (SSE). The LTP tailings solids were also used in humidity cell tests (HCTs) to evaluate constituent leaching under accelerated weathering, and in a controlled static column study to assess potential post-flushing rebound in tailings COC concentrations.

9.1 Tailings Solution Geochemistry

Major ion water quality results show the LTP solution is primarily classified as a Na-SO_4 type water (Figure 11) with elevated pH (≈ 9 to 11) and TDS due to the use of Na_2CO_3, $NaHCO_3$, NaOH, and H_2SO_4 in the milling process (Section 4). The low DO concentrations in some wells (range = 0.14 to 11.4 mg/L) indicate that DO is being consumed by organic decay, producing measurable ammonia (NH_3) from the reduction of nitrate (NO_3^-), and hydrogen sulfide (H_2S) from the reduction of SO_4 (WME, 2020a). The tailings solution contained an average DOC concentration of 13 mg/L which is adequate to produce anoxic conditions (Langmuir, 1997). The presence of NH_3 and H_2S, in conjunction with measurable DO concentrations, indicates the heterogeneous nature of the tailings which contains zones that are both oxidizing and reducing. These zones become mixed during well purging and produce waters containing both measurable DO and reduced chemical species. Measurable DO generally indicates an oxic (>1 mg/L) or suboxic (<1 mg/L) environment, whereas its absence indicates an anoxic environment. Anoxic systems may be with or without measurable H_2S (sulfidic and nonsulfidic). The redox status of the LTP can be categorized as ranging from oxic to suboxic, although the presence of low H_2S concentrations suggests some anoxic sulfidic zones may exist.

Field measured Eh values from the LTP wells ranged from 26 to 464 mV and were compared to the Eh values computed from each of the individual redox couples (H_2O/O_2, Fe^{2+}/Fe^{3+}, NH_4^+/NO_3^-, and H_2S/SO_4^{2-}) (Figure 12). The general poor agreement between measured and computed Eh in groundwater is common and indicates there is no overall system Eh controlling the distribution of all redox-sensitive species. Therefore, Eh should generally be thought of as a qualitative expression of the state of oxidation or reduction in a natural system (Langmuir, 1997). For LTP tailings, the Eh computed from the NH_4^+/NO_3^- redox couple provides the closest match to field-measured Eh values.

Analytical and field results from the tailings wells were evaluated using the geochemical speciation model PHREEQC (Parkhurst and Appelo, 2013) to predict the dissolved forms of U, Se, and Mo in the tailings water. Redox was controlled using the NH_4^+/NO_3^- redox couple and the MINTEQv4.dat database developed by the USEPA was used for all model calculations. The speciation calculations indicate that U occurs primarily as U(VI) in the form of the negatively-charged $UO_2(CO_3)_3^{4-}$ species. Selenium is more easily reduced than U, and under these slightly reducing conditions is predicted to

occur mainly as reduced selenite [Se(IV)] (SeO_3^-), and to a lesser extent oxidized selenate [Se(VI)] (SeO_4^{2-}) in most tailings wells and sumps. Virtually 100% of the dissolved Mo was predicted to occur as the oxidized Mo(VI) molybdate ion (MoO_4^{2-}) in all samples (WME, 2020a).

The concentrations of U, Mo, and Se in the tailings water are potentially controlled by their occurrence as mineral phases. Saturation index (SI) values calculated using PHREEQC show that the LTP solution is undersaturated with respect to the reduced U(IV) minerals (amorphous and crystalline UO_2) due to the very low concentration of U(IV). The concentrations of U(VI) are also insufficient to reach saturation with respect to oxidized U minerals such as carnotite or tyuyamunite. The LTP solution is undersaturated with respect to amorphous elemental Se [Se(am)] and ferroselite ($FeSe_2$), indicating that conditions are not adequately reducing to precipitate reduced Se phases. The SI values for calcium molybdate ($CaMoO_4$) also indicated undersaturated conditions in most samples. The LTP solution is generally oversaturated or in equilibrium with respect to calcite ($CaCO_3$), ferrihydrite [$Fe(OH)_3$(am)], quartz (α-SiO_2), and rhodochrosite ($MnCO_3$), and undersaturated with respect to amorphous aluminum (Al) hydroxide [$Al(OH)_3$(am)] and Fe sulfide (pyrite).

9.2 Tailings Solids Geochemistry

Observations during drilling indicate the tailings solids are heterogeneous and generally consist of alternating and interfingering layers of poorly-graded sands, silts, and clays (WME, 2020a,b). Surface tailings tend to be loose and oxidizing, with increasing moisture and evidence of reducing conditions with depth (dark coloration, odor of H_2S). The tailings mineralogy is dominated by quartz, feldspar, and phyllosilicate clays, with minor calcite and pyrite. The LTP sands contain a higher proportion of quartz and a lower clay content compared to the STP slimes, with an overall bulk mineral composition similar to the alluvium (Figure 13). Visual examination with SEM shows Fe to exist in both reduced and oxidized forms, with an example of goethite (α-FeOOH) replacing pyrite on Figure 13. Although tailings pore waters were calculated to be undersaturated with respect to Se and U minerals, SEM revealed Se in association with Fe on the surface of pyrite and as elemental mineral inclusions. Uranium was associated with Ca and V, consistent with an oxidized mineralogy (tyuyamunite, carnotite) (Figure 13). No solid-phase forms of Mo were identified using XRD or SEM.

The chemical composition of the tailings is consistent with the observed mineralogy and dominated by Al, Ca, Fe, K, and SiO_2. The concentrations of total U, Mo, and Se in tailings ranged from: U (38 to 118 mg/kg), Mo (4 to 19 mg/kg), and Se (79 to 192 mg/kg) (WME, 2020b). A modified SSE technique (WME, 2020a) was used to extract various constituents associated with the following phases: (1) soluble, (2) exchangeable, (3) carbonate bound, (4) Fe/Mn oxide bound, (5) organic/sulfide bound, and (6) residual (Figure 14). Uranium was extracted in various proportions from the soluble, carbonate, Fe/Mn oxide, organic/sulfide, and residual mineral fractions. The soluble fraction represents U in the pore water, and was higher in slimes compared to sands due to their relatively higher porosity and water-holding capacity. Uranium can coprecipitate with calcite and therefore may exist as carbonate-bound U. Uranium released from the organic/sulfide bound fraction may indicate the presence of UO_2 or organically-complexed U. The occurrence of U with titanium and rare earth phosphates observed using SEM (WME, 2020a) or U present as coffinite may constitute the residual fraction. Molybdenum is mainly associated with the residual fraction in sands and the soluble fraction in slimes. The organic/sulfide bound Mo fraction was relatively low, indicating that much of the Mo sulfide that may have been present in the original ore has oxidized. Selenium in the

tailings is mainly associated with the organic/sulfide bound and soluble fractions. The soluble fraction represents the entrained pore water, while the organic/sulfide bound fraction represents oxidation of reduced Se forms identified using SEM. Iron fractionation (Figure 15) is consistent with mineralogical identification of Fe sulfides (pyrite), Fe oxides (goethite, ferrihydrite), resistant Fe oxide minerals (hematite), and aluminosilicate clay minerals containing Fe (WME, 2020a).

The two main forms of sulfur (S) in the tailings are sulfide-S (up to 0.35%) and sulfate-S oxidation products (Figure 16), consistent with the mineralogical identification of pyrite and Fe oxides. The tailings contain elevated pH (up to 10.3), and static ABA results show they are net acid-neutralizing (WME, 2020a). In 20-week duration kinetic tests using HCTs, U, Mo, Se, and SO_4 displayed early concentration spikes in a few tailings leachates, but the overall decreasing trends did not indicate a significant residual source of COCs that would be released upon long-term weathering. The concentration spikes were likely due to delayed flushing/diffusion from the fine-grained material, or possibly from limited oxidation of metal sulfides. The cumulative mass released for U, Mo, and Se showed little to no increase after 20 weeks, indicating that the capacity of the tailings to release COCs had become exhausted. Evaluation of major ion concentration trends in the HCT leachates indicate that rinsing of soluble constituents, dissolution of calcite, and pyrite oxidation are the primary mechanisms controlling the long-term chemistry of weathered tailings solids leachate (WME, 2020a).

9.3 Tailings Rebound Evaluation

Once source control flushing activities at the LTP ceased in 2015 (Section 6), several studies were conducted to assess the potential for post-flushing diffusive mass transfer of COCs from fine-grained materials into the LTP pore water (diffusive rebound). An initial rebound study (Arcadis, 2012) concluded that no future significant diffusive mass transfer and subsequent rebound of COCs is expected to occur. An additional rebound assessment was conducted from 2018 to 2020 through continued monitoring of existing and newly-installed short-screen (5 ft) wells, and with a controlled static column study using undisturbed LTP tailings solids (WME, 2020a). Although some select LTP sumps and existing wells have demonstrated increasing COC concentrations since flushing ceased, results from the short-screen wells indicate either decreasing or overall stable concentrations of COCs and major dissolved constituents in LTP pore water. In addition, results from a controlled static column study provided no indication of diffusive rebound over a 1-yr. test period. The volume-weighted concentrations of U, Mo, and Se in the LTP have also been decreasing since flushing ceased, providing no indication of diffusive concentration rebound in the LTP as a whole (WME, 2020a).

9.4 Alluvial Aquifer Geochemistry

Information regarding detailed water quality, redox conditions, and mineralogy in the alluvial groundwater was collected to understand the controls on COC transport. The major ion water quality signature for the alluvial wells (Figure 17) shows upgradient wells to the north consist of a Ca-SO_4 type water. Wells to the west tend to be dominated by Na-SO_4-type with elevated TDS closest to the LTP due to tailings influence, and become more Ca-SO_4 dominated with distance (WME, 2020a). Wells to the south also tend to be more dominated by Na as the major cation. The alluvial wells underlying the LTP are consistent with a tailings signature due to vertical migration of tailings seepage.

Except for directly beneath the LTP, the alluvial aquifer is more oxidizing compared to the tailings, containing on average higher DO concentrations and low to non-detectable concentrations of Fe^{2+},

Mn^{2+}, NH_3-N, and H_2S (WME, 2020a). Conditions are classified as oxic based on DO concentrations, and speciation calculations using PHREEQC (Parkhurst and Appelo, 2013) indicate the dissolved U, Mo, and Se occur primarily in their oxidized forms: U(VI) as Ca-carbonate complexes ($CaUO_2(CO_3)_3^{2-}$ and $Ca_2UO_2(CO_3)_3$), Mo(VI) as the molybdate ion (MoO_4^{2-}), and Se(VI) as the selenate ion (SeO_4^{2-}). The SI values for the reduced U minerals (UO_2) indicate a high degree of undersaturation due to the low calculated proportion of U(IV), and the groundwaters are also undersaturated with respect to the common oxidized U(VI) minerals (carnotite, tyuyamunite), elemental Se, ferroselite ($FeSe_2$), and powellite ($CaMoO_4$). The alluvial aquifer is in equilibrium with calcite, oversaturated with respect to ferrihydrite, and undersaturated with respect to pyrite.

Although the tailings solution and the alluvial groundwater are both undersaturated with respect to powellite ($CaMoO_4$), groundwater beneath and adjacent to the LTP tends to be oversaturated or in equilibrium with respect to powellite (Figure 18). Powellite is known to be an important sink for Mo under neutral pH to alkaline conditions, where it forms as coatings on carbonate and silicate minerals (Frascoli and Hudson-Edwards, 2018). As the Na-SO_4 seepage with elevated Mo migrates into the underlying Ca-SO_4 alluvial aquifer, the groundwater reaches saturation with respect to powellite:

$$Ca^{2+}(aq) + MoO_4^{2-}(aq) \rightleftharpoons CaMoO_4(s) \quad [4]$$

Powellite can also exist in equilibrium with calcite (Lindsay, 1979):

$$CaCO_3(s) + H^+(aq) + MoO_4^{2-}(aq) \rightleftharpoons CaMoO_4(s) + HCO_3^-(aq) \quad [5]$$

Because its formation is kinetically limited (Frascoli and Hudson-Edwards, 2018), powellite is initially oversaturated and becomes closer to equilibrium (saturation index =0) a short distance from the LTP (Figure 18). The steep Mo concentration gradient near the LTP, coupled with the historical limited migration of Mo at the Site, is more consistent with Mo precipitation rather than adsorption.

9.5 Alluvial Solids Geochemistry

Mineralogy results show the alluvial aquifer is dominated by quartz, feldspar, and calcite (Figure 13). Lower quantities of clay were present (2 to 15% kaolinite, smectite, illite) and the cation exchange capacity (CEC) was low (2.9 to 7.7 $cmol_+/kg$). Pyrite was below detection using XRD (<1%), consistent with the low measured total-S and non-detectable sulfide-S (Figure 16). Natural weathering in a predominantly oxidizing environment limits the preservation of Fe sulfides, however pyrite has been identified in alluvial samples containing a higher content of silts and clays (HMC, 2018). Weathering of pyrite and other Fe-bearing minerals generates Fe oxides as stable weathering products under oxidizing conditions. Iron oxides are considered the most important adsorbents for trace elements in nature due to their high adsorption capacity and their tendency to be finely dispersed and to occur as mineral coatings (Dzombak and Morel, 1990; Langmuir, 1997). Iron oxides are undoubtedly present but were not identified using XRD because crystalline forms were below the XRD detection limit (1 to 3%) and/or a significant fraction of the Fe oxide is non-crystalline (ferrihydrite). Hematite has previously been identified in the alluvium (HMC, 2018), and SSE results for the WME (2020a) samples (Figure 15) indicate a ferrihydrite content ranging from 0.057% to 0.23% as Fe. Additional samples collected in 2019 indicate a ferrihydrite content of 0.01 to 0.38% as Fe (WME, 2020b). The mean ferrihydrite content for all alluvium samples (N=27) is 0.14% as Fe.

Solution speciation results indicated that U, Mo, and Se in the alluvial groundwater occur as negatively-charged oxyanions (Section 9.4), and thus the SSE procedure was subsequently revised to replace the exchangeable step ($MgCl_2$) with a $NaHCO_3$ extraction to recover adsorbed constituents (WME, 2020b). The sum of the adsorbed plus Fe/Mn oxide fraction is assumed to represent the total fraction of U, Mo, and Se associated with ferrihydrite, where the $NaHCO_3$ step removes the adsorbed species from the mineral surface, and the Fe/Mn oxide fraction releases species coprecipitated within the Fe oxide structure. The SSE results for U, Mo, and Se in samples of alluvium collected from below the STP and LTP are shown on Figure 19. A significant fraction of U is water soluble and the remaining U is associated with the adsorbed plus Fe/Mn oxide and carbonate bound fractions. A relatively larger percentage of the Mo was water soluble with the remaining being dominated by the adsorbed plus Fe/Mn oxide and residual fractions. A larger proportion of the Se was organic/sulfide bound which reflects the immobilization of Se due to slightly reducing conditions below the tailings.

9.6 Attenuation Mechanisms

Potential attenuation mechanisms for the COCs in the Alluvial Aquifer include: (1) direct mineral precipitation, (2) coprecipitation with existing alluvial minerals, (3) adsorption by clay minerals, and (4) adsorption by ferrihydrite. Direct precipitation is not considered an important attenuation mechanism due to the extent of undersaturation with respect to the oxidized mineral forms. However, U may be partially controlled by coprecipitation with calcite (Section 9.5).

The affinity for adsorption of COCs by clay minerals and ferrihydrite is controlled by their dissolved forms in groundwater and the surface charge of the mineral, both of which are pH-dependent. Uranium is mainly present as negatively-charged complexes ($CaUO_2(CO_3)_3^{2-}$) and would only exist as positively-charged species (UO_2OH^+, UO_2^{2+}) below pH of 6 (Figure 20a). Similarly, Mo occurs primarily as the negatively charged MoO_4^{2-} ion under Site pH conditions (pH ≈ 7) (Figure 20b). Selenium speciation is similar to Mo and occurs primarily as selenate (SeO_4^{2-}) (WME, 2020a). Clay minerals are negatively-charged above pH of 5 (Appelo and Postma, 2013), producing a swarm of positively-charged cations (Na^+, Ca^{2+}) at their surface, where the concentrations of negatively-charged anions are the lowest. A diffuse layer of ions extends from the surface into the solution, with cations at higher and anions at lower concentrations than in the solution (Figure 21). Major cations are held rather weakly to the clays by electrostatic force, whereas dissolved metals have the potential to bond more strongly with oxygen groups on mineral surfaces. However, the anionic forms of U, Mo, and Se would be essentially excluded from interacting with negatively-charged clays (Figure 21).

Alternatively, ferrihydrite surfaces will be neutral or positively-charged under most groundwater pH conditions (Appelo and Postma, 2013). Oxyanion adsorption to ferrihydrite involves both an electrostatic attraction and chemical bonding to the mineral surface, and is considered to be the primary mechanism for partitioning of the primary COCs in the alluvial aquifer (Figure 22). The extent of adsorption is not 100%, and will vary depending on the specific constituent and local geochemical conditions, such that a fraction of the COCs remains mobile. Due to its widespread nature, studies have shown ferrihydrite to exert more control on the attenuation of U compared to clays. For example, U adsorption data compiled by the USEPA (1999) suggests that soils containing higher percentages of Fe oxides, mineral coatings, and/or clay minerals will exhibit higher adsorption capacities compared to soils solely dominated by quartz and feldspars (Figure 23). Some investigators have also shown that adsorption capacities for soils of mixed mineralogy are not

necessarily correlated with clay content, but rather U appeared to be associated with mineral surface coatings of variable pH, consistent with ferrihydrite occurrence (USEPA, 1999).

The USDOE (2014) presented an analogous conceptual model of U transport in the Rio San Jose alluvium. The Rio San Jose is predominantly oxidizing and geochemical modeling indicated U mineral precipitation is not a mechanism controlling groundwater transport. The conceptual geochemical model assumed the majority of U exists as oxidized U(VI) whose transport is primarily controlled by pH-dependent adsorption to ferrihydrite. Geochemical modeling was then used to evaluate the potential effects of alkalinity and pH on U transport. The predicted concentrations (Figure 24) demonstrate the variability in extent of U adsorption as affected by both alkalinity and pH, and ultimately controlled by corresponding changes in U speciation (Figure 20a). At pH <4.5, U is primarily dissolved. From a pH of about 5 to 7.5 with low alkalinity, U is more strongly adsorbed. At pH is > 8, U is primarily dissolved under moderate alkalinity concentrations.

The concentrations of Mo in the alluvial groundwater are limited to around 0.1 to 1 mg/L in the direct vicinity of the LTP (HMC and HE, 2020) due to precipitation as powellite (Section 9.4). Dissolved Mo which continues to migrate through the alluvium exists as primarily as molybdate (MoO_4^{2-}). Studies have shown that molybdate adsorption onto ferrihydrite is maximized between pH of 4 to 5, but decreases rapidly with increasing pH, with minimal adsorption above pH 7 to 8 (Figure 25a). Similar to U, ferrihydrite has been shown to be a more efficient adsorbent of Mo compared to common clay minerals under equal pH conditions (Goldberg et al., 1996). Therefore, it is expected that under Site pH conditions (pH ≈ 7), Mo will migrate as MoO_4^{2-} in the alluvial aquifer with minimal adsorption by Fe oxide or clay minerals in the alluvial aquifer.

Selenate (SeO_4^{2-}) exhibits maximum adsorption to ferrihydrite in the pH range of 2 to 4, but there is a rapid decrease in adsorption between pH 6 and 7.5, with minimal adsorption above pH 8.5 (Figure 25b). As for U and Mo, ferrihydrite is also a more efficient adsorbent of Se compared to common clay minerals (Goldberg, 2014). Selenite (SeO_3^{2-}) exhibits a maximum adsorption up to pH 8, where the extent of adsorption decreased rapidly with increasing pH above 8 (Goldberg, 2012). Most alluvial aquifer samples have a pH greater than 6, and thus Se will not be completely attenuated because selenate is predicted to be the predominant form. It has been recognized that the presence of reduced microenvironments may exist which could produce locally-reducing conditions (HMC, 2018). Selenium is more easily reduced relative to U and Mo, and thus could also potentially migrate less conservatively as selenite, or precipitate as Se(IV) if reducing conditions are encountered.

10.0 CONCEPTUAL GEOCHEMICAL MODEL

A summary of the resulting Site conceptual geochemical model (CGM) for the Grants Reclamation Project is illustrated on Figure 26 and was developed using historic information along with results from the recent characterization studies (WME, 2020a,b). In the current CGM, an active source term is contained within a dissipating mound of tailings water where the rates of seepage will continue to decrease over time. Due to the milling process, the active source term is an alkaline (pH ≈ 10) Na-SO_4 to Na-HCO_3 type water, with elevated concentrations of TDS, COCs, and indicator constituents (Cl and SO_4). Tailings redox conditions range from oxic to suboxic with the primary COCs occurring as oxyanions (MoO_4^{2-}, SeO_3^{2-}, $UO_2(CO_3)_3^{4-}$) which tend to remain soluble. Due to the onset of reducing conditions within and beneath the LTP, Se concentrations have been decreasing over time.

A minor residual source term contains those solid-phase forms of COCs with the potential for release into infiltrating water following tailings drain down, either through weathering of pyrite, elemental Se, MoS_2, and secondary U minerals, or through diffusive rebound following LTP flushing. Static testing has shown the tailings are non-acid generating due to the excess acid neutralizing capacity. The HCT results indicate no significant release of Fe, SO_4, acidity, or COCs upon accelerated weathering, such that the long-term COC concentrations are not expected to significantly increase in the infiltrating water. In addition, the overall concentrations of U, Mo, and Se in the LTP seepage have been decreasing since flushing ceased, providing no indication of diffusive concentration rebound.

Dissolved COCs migrate with the tailings seepage both vertically and horizontally into the underlying SMC Alluvial Aquifer, and becomes partially diluted as it mixes with oxidizing Ca-SO_4 type water from upgradient. As the tailings-influenced groundwater moves downgradient, the conservative indicator constituents (Cl, SO_4) are controlled by dilution and dispersion. Uranium becomes dominated by U(VI)-calcium complexes ($CaUO_2(CO_3)_3^{2-}$), selenate (SeO_4^{2-}) becomes the main form of Se, and Mo remains as the molybdate ion (MoO_4^{2-}). These forms of dissolved COCs which are bonded with oxygen and negatively-charged are collectively referred to as oxyanions and are generally mobile in the groundwater environment. In the immediate vicinity of the LTP, however, mixing of tailings seepage with Ca-SO_4 groundwater and reaction with calcite in the alluvium causes powellite to precipitate, limiting the concentration of Mo to between 0.1 and 1 mg/L outside of the LTP. The oxyanionic forms of the COCs are only partially attenuated by ferrihydrite adsorption to varying degrees, depending on factors such as pH, alkalinity, TDS, and the presence of competing adsorbing species. Some areas of the groundwater may be slightly reducing, such that selenate may be reduced to selenite or perhaps precipitate as elemental Se. The fraction of COCs which remain in solution continue to migrate downgradient as oxyanions, and are eventually attenuated to concentrations below Site standards through additional groundwater mixing, dilution, and limited adsorption to mineral surfaces. The CGM presented here provides a basis for ongoing development of computational geochemical models to predict post-closure transport of COCs in the SMC Alluvial Aquifer.

11.0 REFERENCES

Abdelouas, A. 2006. Uranium Mill Tailings: Geochemistry, Mineralogy, and Environmental Impact. Elements. Volume 2:335-341. December.

Appelo, C.A.J. and D. Postma. 2013. Geochemistry, Groundwater, and Pollution. Second Edition. A.A. Balkema, The Netherlands. 649 pp.

Agency for Toxic Substances and Disease Registry (ATSDR). 2009. Health Consultation: Homestake Mining Company Mill Site. Milan, Cibola County, New Mexico. June 26.

Arcadis. 2012. Rebound Evaluation Summary Report. Prepared for Homestake Mining Company of California. December.

Brown and Caldwell. 2018. San Mateo Creek Basin and HMC Mill Hydrogeologic Site Conceptual Models. Prepared for Homestake Mining Company of California. January 8.

Butler, R.D. 1972. Carbonate Leaching of Uranium Ores: A Review. pp. III-1 through III-13. In Uranium Processing: Papers from the AAEC Symposium on Uranium Processing Held at Lucas Heights, July 20-21. Australian Atomic Energy Commission.

Chavez, E.A. 1961. Progress Report on Contamination of Potable Ground Water in the Grants-Bluewater Area, Valencia County, New Mexico. New Mexico State Engineers Office, Roswell, New Mexico.

Coleman, R.G. and Delevaux, M. 1957. Occurrence of Selenium in Sulfides from Some Sedimentary Rocks of the Western United States. Economic Geology. 52:499-527.

D'Appolonia Consulting Engineers, Inc. (D'Appolonia). 1980. Engineer's Report: Stability Assessment. Uranium Mill Tailings Pond, United Nuclear-Homestake Partners. Grants, New Mexico.

Dzombak, D.A. and F.M.M. Morel. 1990. Surface Complexation Modeling: Hydrous Ferric Oxide. John Wiley & Sons, New York. 393 pp.

Frascoli, F. and K.A. Hudson-Edwards. 2018. Geochemistry, mineralogy, and microbiology of molybdenum in mining-affected environments. Minerals. 8(2):42.

GEOCHEM, 1992. Geochemical Analysis of Mill Tailings from Homestake Mining Company Grants Uranium Mill. Prepared for AK GeoConsult, Inc. Albuquerque, New Mexico. October 1.

Goldberg, S., H.S. Forster, and C.L. Godfrey. 1996. Molybdenum adsorption on oxides, clay minerals, and soils. Soil Science Society of America Journal. 60:425-432.

Goldberg, S. 2009. Influence of soil solution salinity on molybdenum adsorption by soils. Soil Science. 174:9-13).

Goldberg, S. 2012. Modeling selenite adsorption envelopes on oxides, clay minerals, and soils using the ripple layer model. Soil Science Society of America Journal. 77:64-71.

Goldberg, S. 2014. Modeling selenate adsorption behavior on oxides, clay minerals, and soils using the triple layer model. Soil Science. 179:568-576.

HDR. 2020. Final Remedial Investigation Report. Homestake Mining Superfund Site. March 30th.

Homestake Mining Company of California (HMC). 1982. State of New Mexico Environmental Improvement Division Uranium Improvement Division Uranium Mill License Renewal Application Environmental Report. Three Volumes.

Homestake Mining Company of California (HMC). 2018. Evaluation of Water Quality in Regard to Site Background Standards at the Grants Reclamation Project. Prepared by Arcadis U.S., Inc. (Highlands Ranch, CO). September.

Homestake Mining Company of California (HMC). 2019. Groundwater Corrective Action Program. Prepared for the U.S. Nuclear Regulatory Commission. December.

Homestake Mining Company of California (HMC) and Hydro-Engineering LLC (HE). 2020. 2019 Annual Monitoring Report / Performance Review for Homestake's Grants Project Pursuant to NRC License SUA-1471 and Discharge Plan DP-200. Prepared for the U.S. Nuclear Regulatory Commission and New Mexico Environment Department. March.

Hydro-Engineering (HE). 1983. Ground-Water Discharge Plan for Homestake's Mill Near Milan, New Mexico. Prepared for Homestake Mining Company. June.

Hydro-Engineering (HE). 2019. Mixing Model Modifications and Predictions. March 12.

International Engineering Company (IECO). 1977. Stability Analysis: Uranium Tailings Pond. Prepared for United Nuclear-Homestake Partners.

Kauffman, R.F., G.G. Eadie, and C.R. Russell. 1976. Effects of Uranium Mining and Milling on Ground Water in the Grants Mineral Belt, New Mexico. Ground Water, 14:296-308.

Landa, E. 1980. Isolation of Uranium Mill Tailings and Their Component Radionuclides from the Biosphere-Some Earth Science Perspectives. Geological Survey Circular 814. U.S. Geological Survey, Arlington, VA. 32 pp.

Langmuir, D. 1997. Aqueous Environmental Chemistry. Prentice Hall, NJ. 600 pp.

Lee, J.Y. and J.I. Yun. 2013 Formation of ternary $CaUO_2(CO_3)_3^{2-}$ and $Ca_2UO_2(CO_3)_3(aq)$ complexes under neutral to weakly alkaline conditions. Dalton Transactions. 42:9862-9869.

Lindsay, W.L. 1979. Chemical Equilibria in Soils. John Wiley & Sons, NY. 449 pp.

McLemore, V. 2007. Uranium Resources in New Mexico. SME Annual Meeting, February 25-28. Denver, CO. Preprint 07-111.

Nash, J.T., H.C. Granger, and S.S. Adams. 1981. Geology and Concepts of Genesis of Important Types of Uranium Deposits. Economic Geology. 75th Anniversary Volume. 63-116.

National Academy of Sciences (NAS). 1986. Scientific Basis for Risk Assessment and Management of Uranium Mill Tailings. National Academy Press, Washington D.C.

New Mexico Health and Environment Department (NMHED). 1980. Water Quality Data for Discharges from New Mexico Uranium Mines and Mills. July.

Parkhurst, D.L. and C.A.J. Appelo. 2013. Description of Input and Examples for PHREEQC Version 3 - A Computer Program for Speciation, Batch-Reaction, One-Dimensional Transport, and Inverse

Geochemical Calculations: U.S. Geological Survey Techniques and Methods, Book 6, Chap. A43, 497 p., available only at http://pubs.usgs.gov/tm/06a43.

Rosenzweig, A. 1961. Mineralogical Notes on the Uranium Deposits of the Grants and Laguna District, New Mexico. New Mexico Geological Society 12th Annual Fall Field Conference Guidebook. pp. 168-171.

Skiff, K.E. and J.P. Turner. 1981. A Report on Alkaline Carbonate Leaching at Homestake Mining Company. November 12.

Smedley, P.L. and D.G. Kinniburgh. 2017. Molybdenum in natural waters: A review of occurrence, distributions and controls. Applied Geochemistry. 84:387-432.

Thamm, J.K., A.A. Kovschak, Jr., and S.S. Adams. 1980. Geology and Recognition Criteria for Sandstone Uranium Deposits of the Salt Wash Type, Colorado Plateau Province.

United States Department of Energy (USDOE). 2014. Site Status Report: Groundwater Flow and Contaminant Transport in the Vicinity of the Bluewater, New Mexico, Disposal Site. November.

United States Environmental Protection Agency (USEPA). 1975. Impact of Uranium Mining and Milling on Water Quality in the Grants Mineral Belt, New Mexico. EPA 906/9-75-002. USEPA Region 6, Dallas, Texas. September.

United States Environmental Protection Agency (USEPA). 1999. Understanding Variation in Partition Coefficient, Kd, Values. Volume 2: Review of Geochemistry and Available K_d Values for Cadmium, Cesium, Chromium, Lead, Plutonium, Radon, Strontium, Thorium, Tritium (^3H), and Uranium. EPA 402-R-99-004B. USEPA, Washington, D.C. August.

United States Nuclear Regulatory Commission (USNRC). 2003. Standard Review Plan for the Review of a Reclamation Plan for Mill Tailings Sites Under Title II of the Uranium Mill Tailings Radiation Control Act of 1978. NUREG-1620. USNRC, Washington, D.C.

Worthington Miller Environmental LLC (WME). 2020a. Geochemical Characterization of Tailings, Alluvial Solids and Groundwater, Grants Reclamation Project. Prepared for Homestake Mining Company. May.

Worthington Miller Environmental LLC (WME). 2020b. 2019 Supplemental Tailings and Alluvial Characterization Study, Grants Reclamation Project. Prepared for Homestake Mining Company. April.

Tables

Table 1: Chemical Characteristics of Homestake Mill Tailings Solution.

Constituent	Tailings Solution[1] (HE, 1983)				Tailings Sump (NMHED, 1980)			Average	
	11-16-78	11-6-79	9-23-81	10-28-82	10-26-77	11-16-78	11-6-79	Solution	Sump
Calcium	<0.01	<0.01	135	35	nr[2]	10.0	60.0	85	35
Magnesium	nr	<0.1	30.0	nr	nr	nr	813	30.0	813
Sodium	10,000	10,000	9,800	9,080	6,141	8,464	9,292	9,720	7,966
Potassium	0.58	nr	nr	450	nr	31.2	35.1	225	33.2
Bicarbonate	3,280	nr	1,850	2,480	nr	nr	2,388	2,537	2,388
Carbonate	nr	nr	6,450	nr	nr	nr	nr	6,450	--------
Sulfate	8,100	8,420	15,700	12,800	5,532	8,346	8,412	11,255	7,430
Chloride	624	1,070	2,340	1,870	793.2	1,014	1,418	1,476	1,075
TDS	nr	nr	43,300	31,400	17,035	20,710	25,400	37,350	21,048
pH	nr	10.1	10.3	9.9	10.12	nr	10.32	10.1	10.22
Nitrate-N	13.8	11.0	8.2	nr	nr	22.42	10.72	11.0	16.6
Ammonia-N	<1.0	nr	nr	nr	11.2	13.9	17.8	<1.0	14.3
Aluminum	nr	nr	<1.0	nr	nr	nr	<0.25	<1.0	<0.25
Arsenic	0.18	nr	0.07	0.08	2.86	7.19	5.02	0.11	5.02
Barium	<1.0	nr	<1.0	<1.0	<0.10	0.051	<0.10	<1.0	0.051
Cadmium	<0.01	nr	<0.01	<0.01	nr	0.0277	0.001	<0.01	0.014
Lead	<0.01	nr	<0.01	0.01	nr	<0.005	0.007	<0.01	0.007
Molybdenum	80.5	74.8	105	94.0	72.0	105.2	104.5	88.6	93.9
Selenium	26.4	14.7	35.5	24.8	51.18	31.16	27.88	25.4 (*0.92*)[3]	36.7
Uranium	54.3	47.3	21.0	24.7	44.0	52.8	4.17	36.8 (*150*)[3]	33.7
Vanadium	16.9	nr	9.23	4.23	nr	13.6	1.18	10.1 (*6.8*)[3]	7.39
Zinc	14.8	nr	6.62	<1.0	nr	<0.10	<0.25	10.7	----------
Gross Alpha (pCi/L)	nr	nr	nr	nr	nr	10,000 ±1,000	3,400±400	29,000	6,700
^{226}Radium (pCi/L)	31.9	23.5	88.4	80.3	58 ±4	90 ±1	56 ±17	56.0 (*52*)[3]	68
^{210}Lead (pCi/L)	nr	nr	nr	nr	49 ±8	nr	nr	-------	49 ±8
^{230}Thorium (pCi/L)	nr	0.036	0.151	nr	nr	nr	nr	0.094	0.094

[1] All concentrations are total (unfiltered) and expressed as mg/L except where noted. [2] nr = not reported. [3] Average value reported by USEPA, 1975.

Figures

Figure 1: Location of the Homestake Mining Company Grants Reclamation Project.

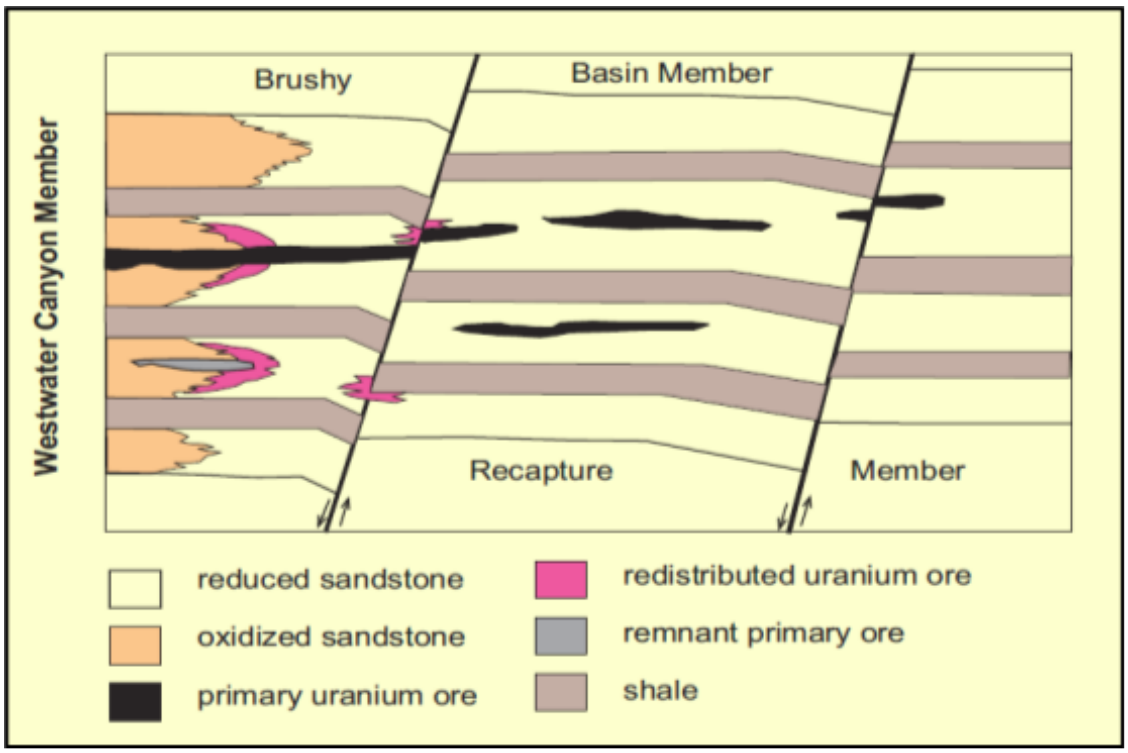

Figure 2: Uranium Deposits Found in the Morrison Formation (McLemore, 2007).

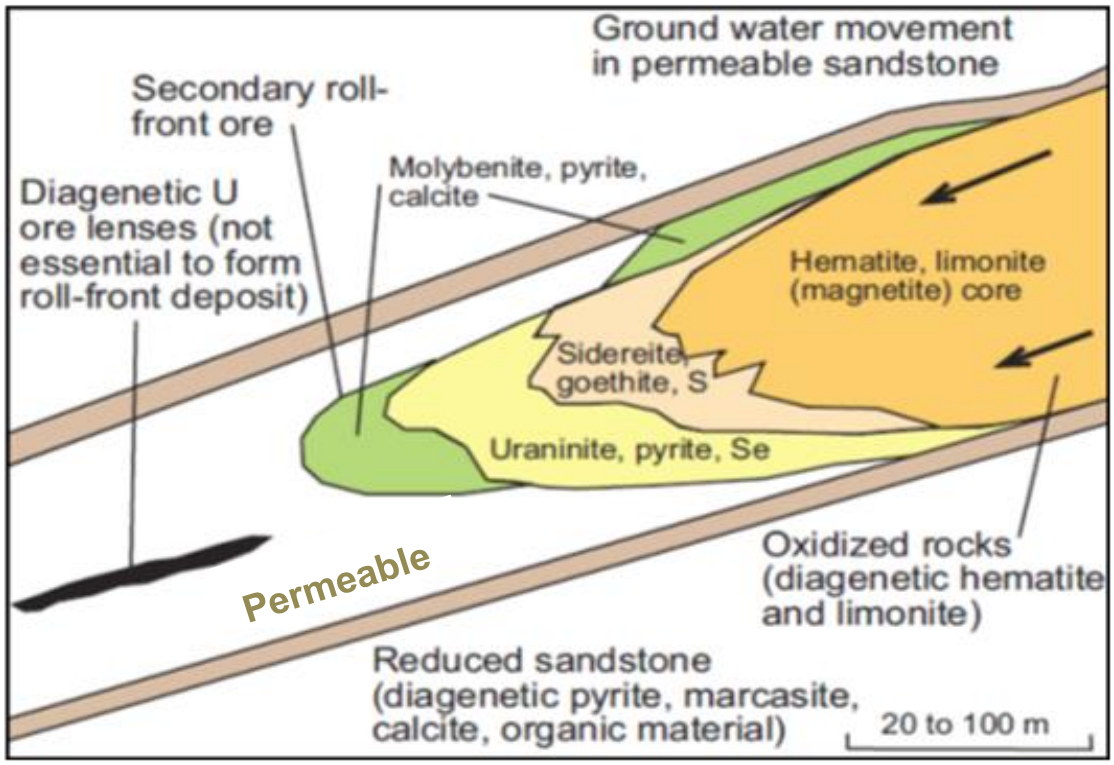

Figure 3: Formation of a Redistributed Sandstone U Deposit (McLemore, 2007).

Figure 4: UN-HP Mill During Active LTP Tailings Deposition.

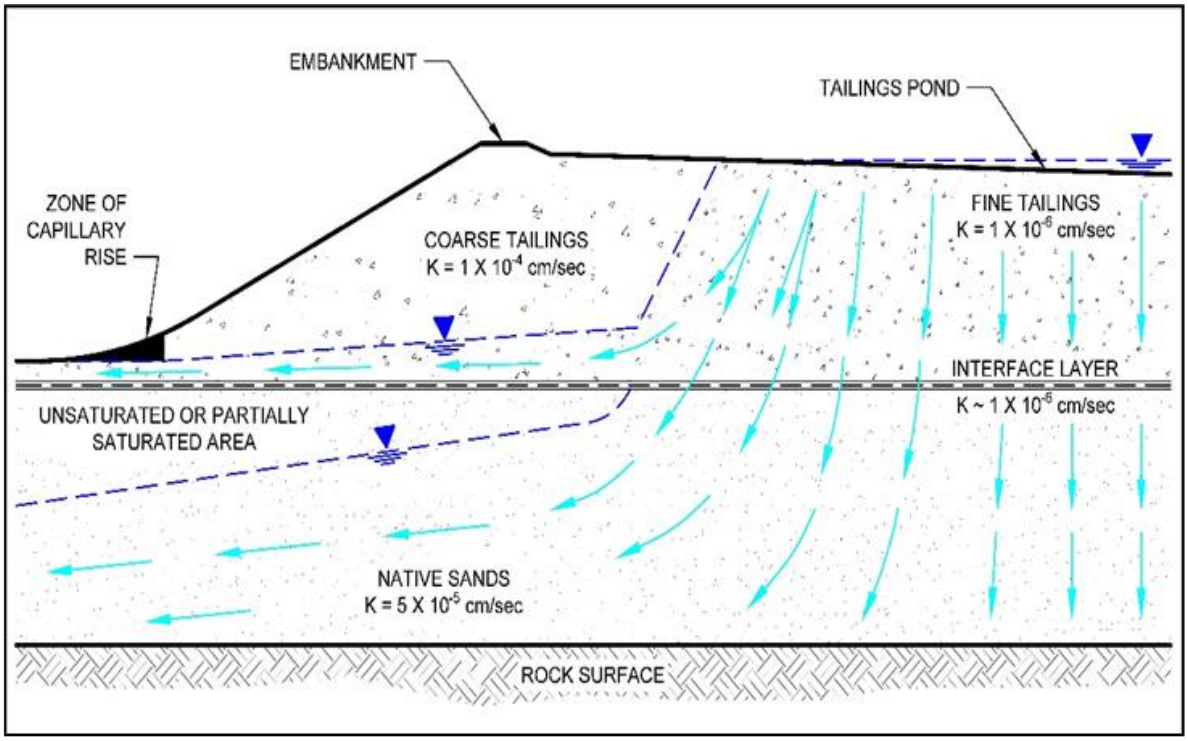

Figure 5: Conceptual Flow Regime in the LTP Embankment (D'Appolonia, 1980).

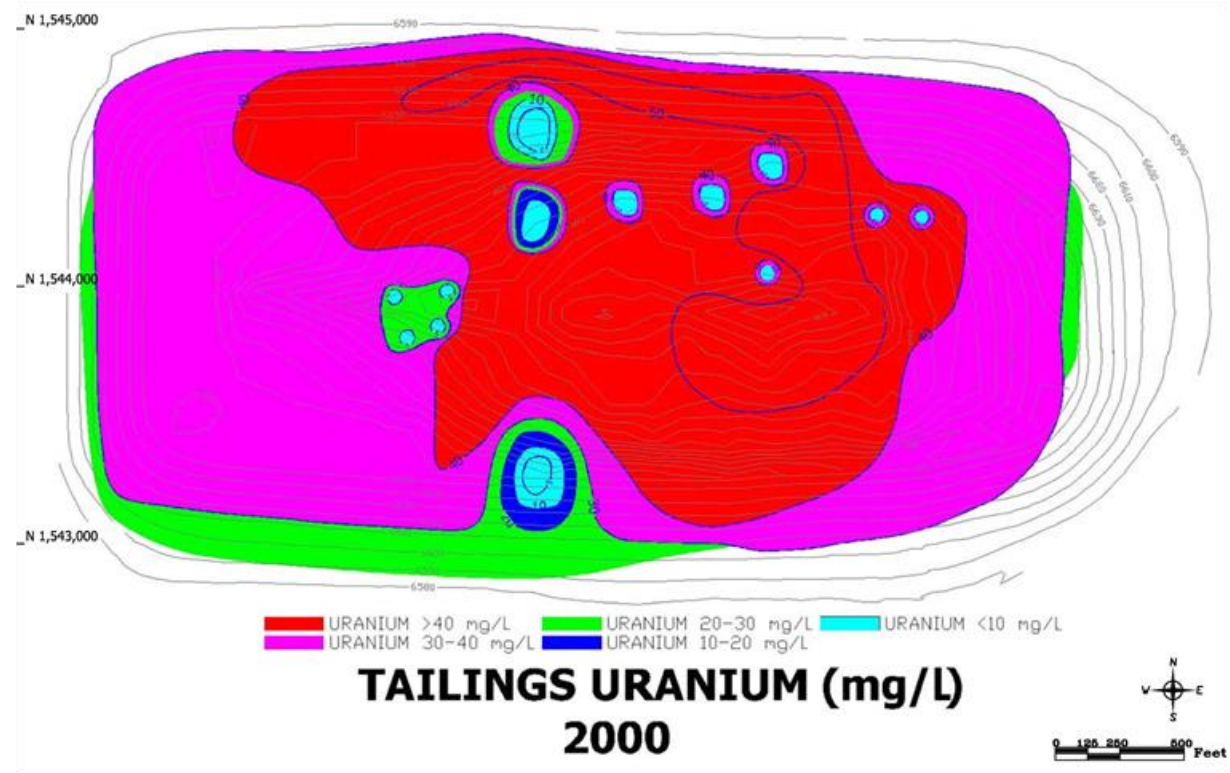

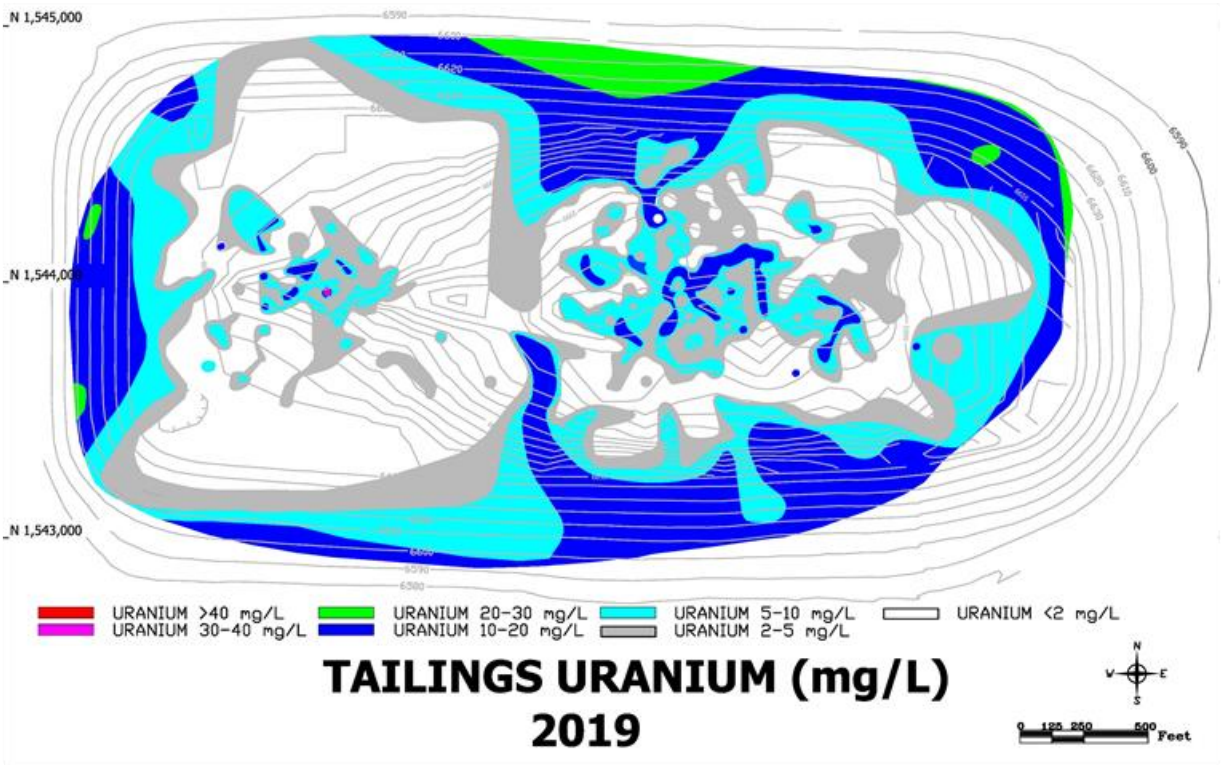

Figure 6: Changes in LTP U concentrations, 2000 and 2019 (HMC and HE, 2020).

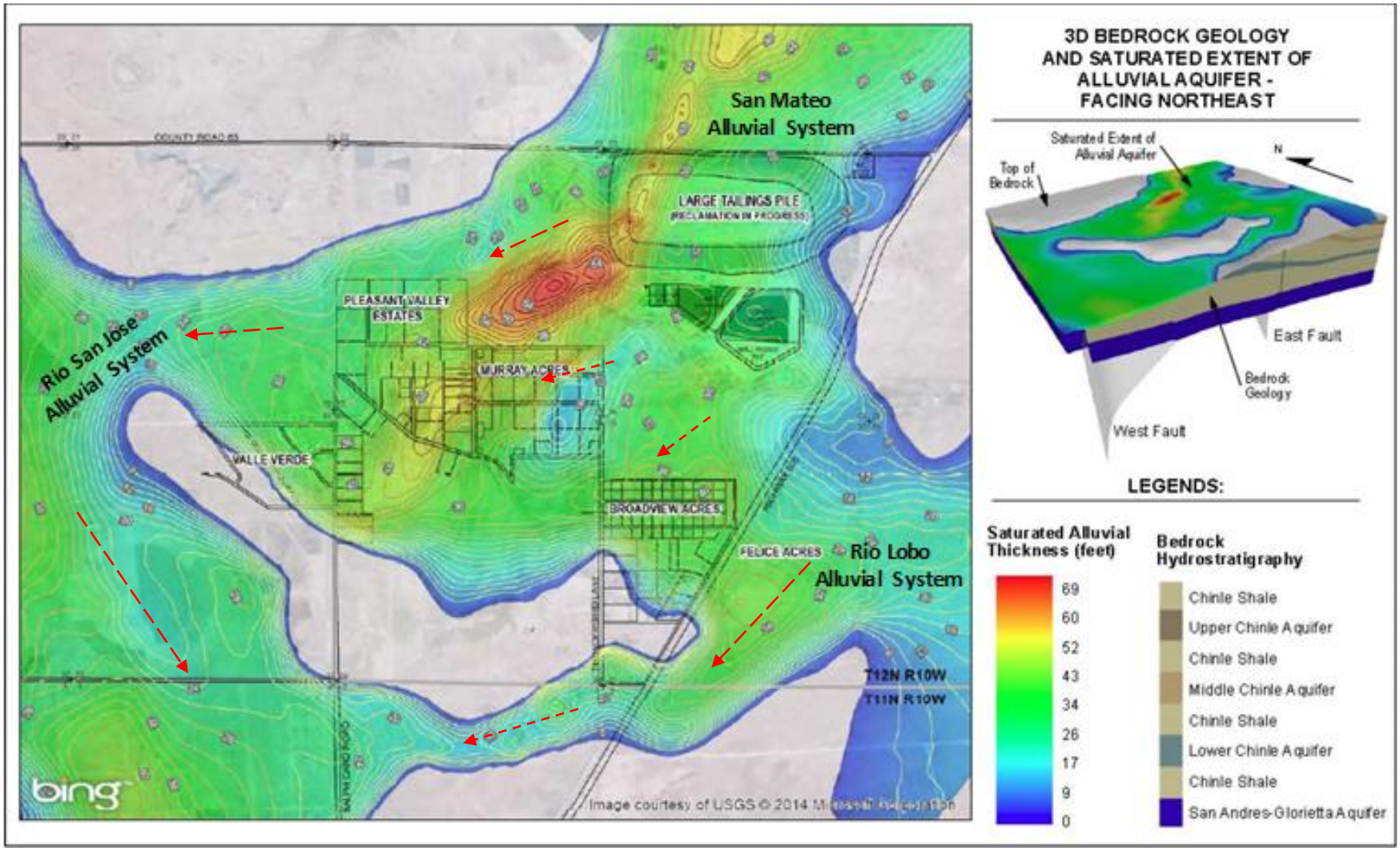

Figure 7: Saturated Extent of the Alluvial Aquifer With General Flow Directions (HDR, 2020).

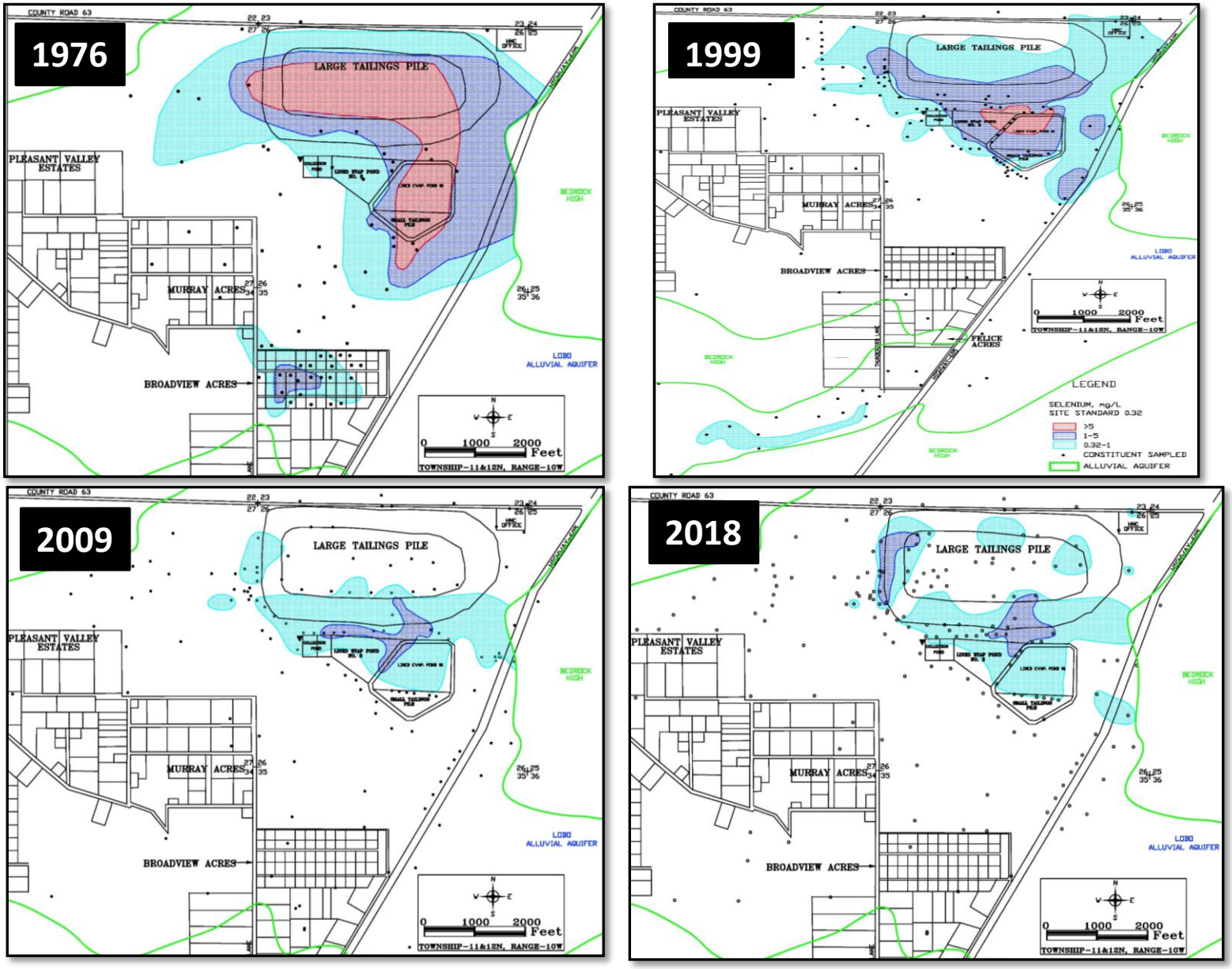

Figure 8: Selenium Plume History in the Alluvial Aquifer (HMC, 2019).

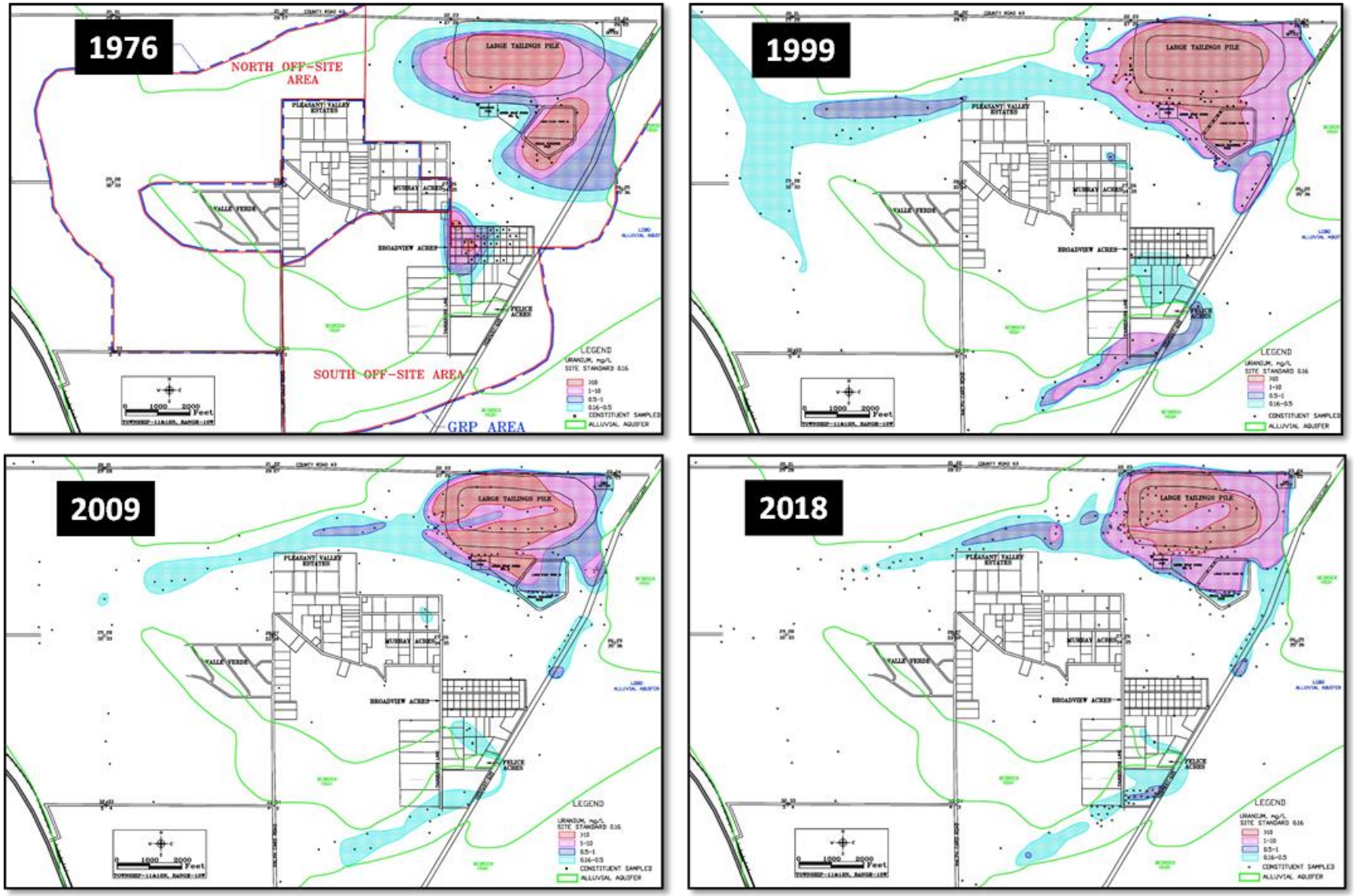

Figure 9: Uranium Plume History in the Alluvial Aquifer (HMC, 2019).

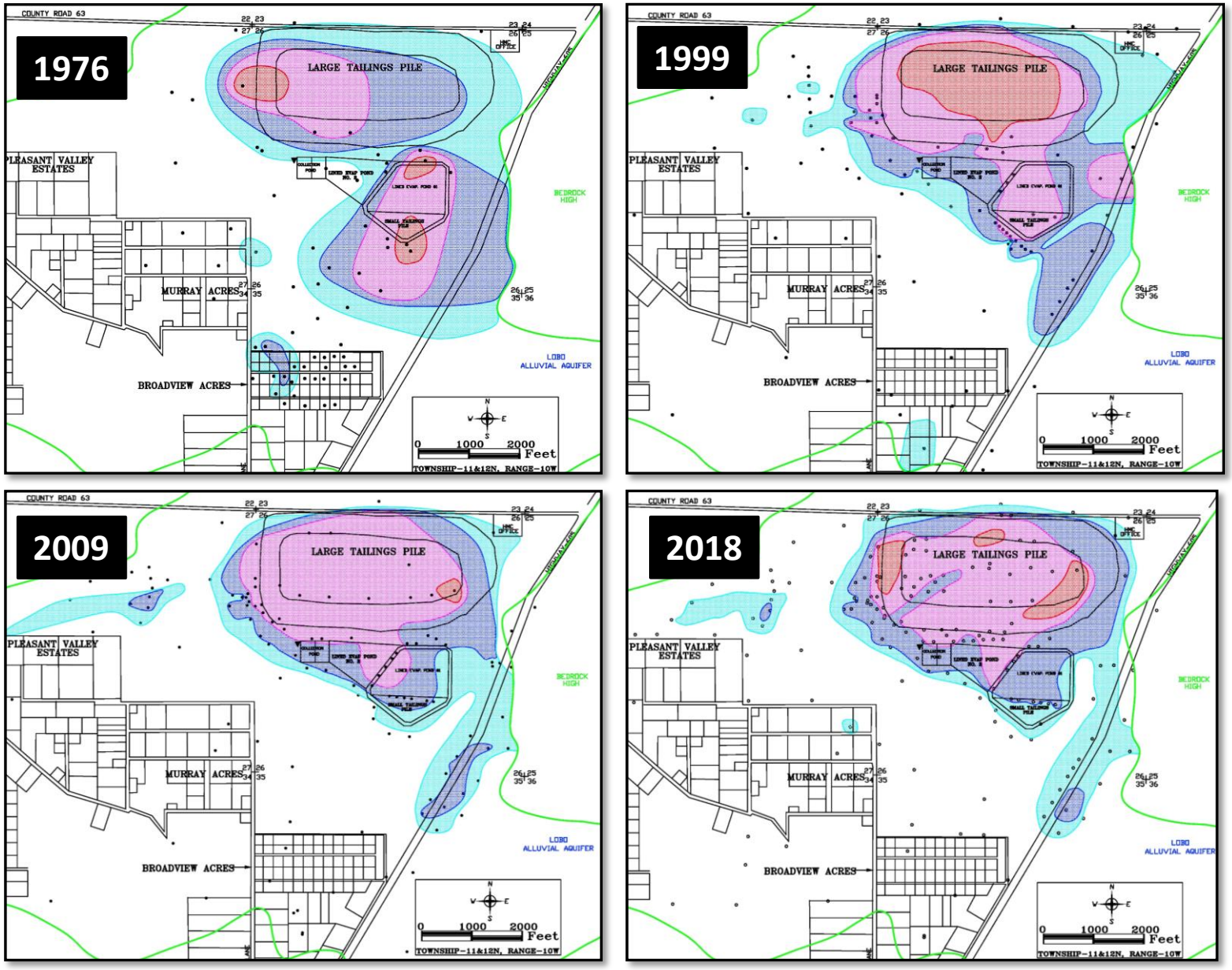

Figure 10: Molybdenum Plume History in the Alluvial Aquifer (HMC, 2019).

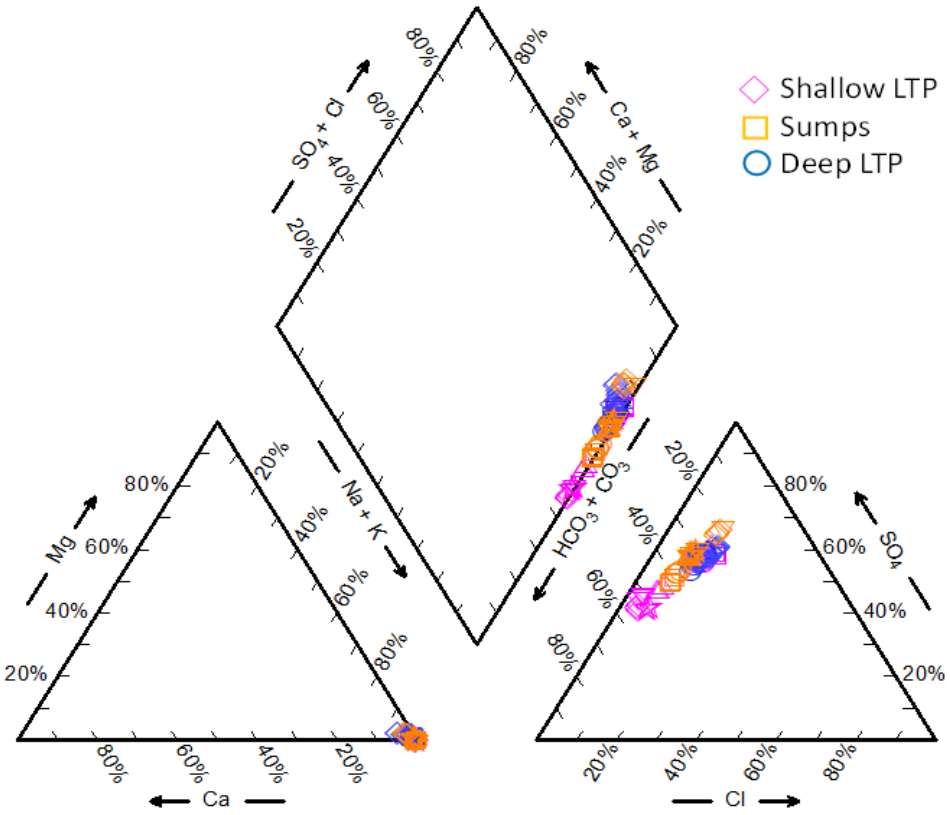

Figure 11: Trilinear Diagram for the LTP Wells and Sumps.

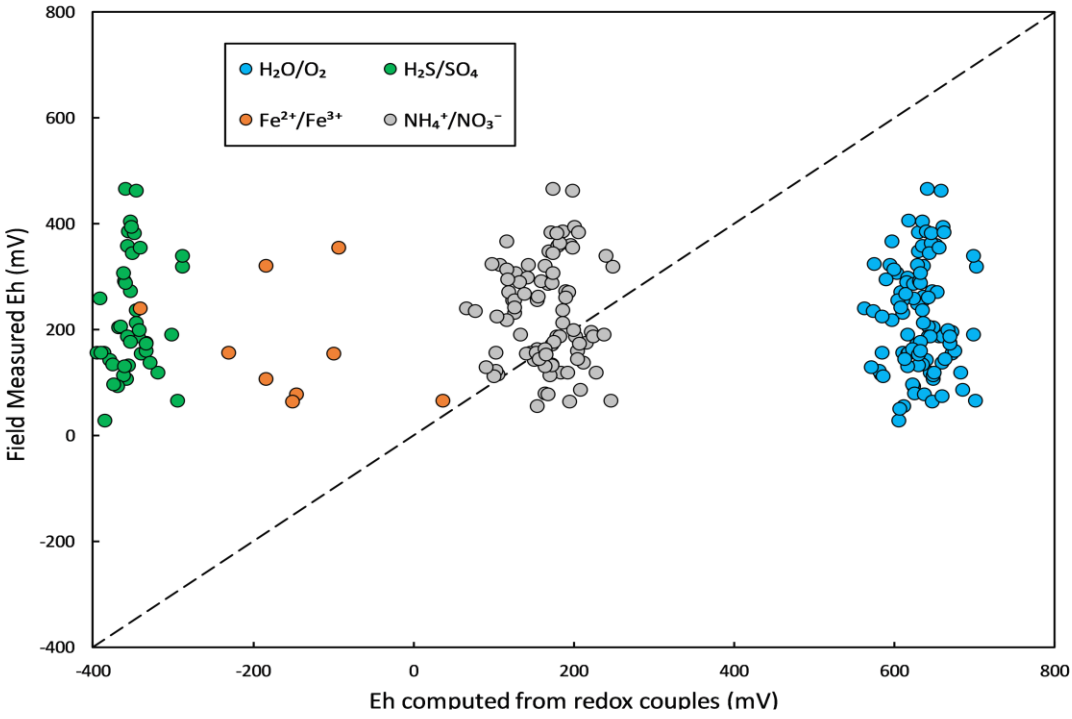

Figure 12: Field Eh vs. Computed Eh for Redox Couples in LTP Wells and Sumps.

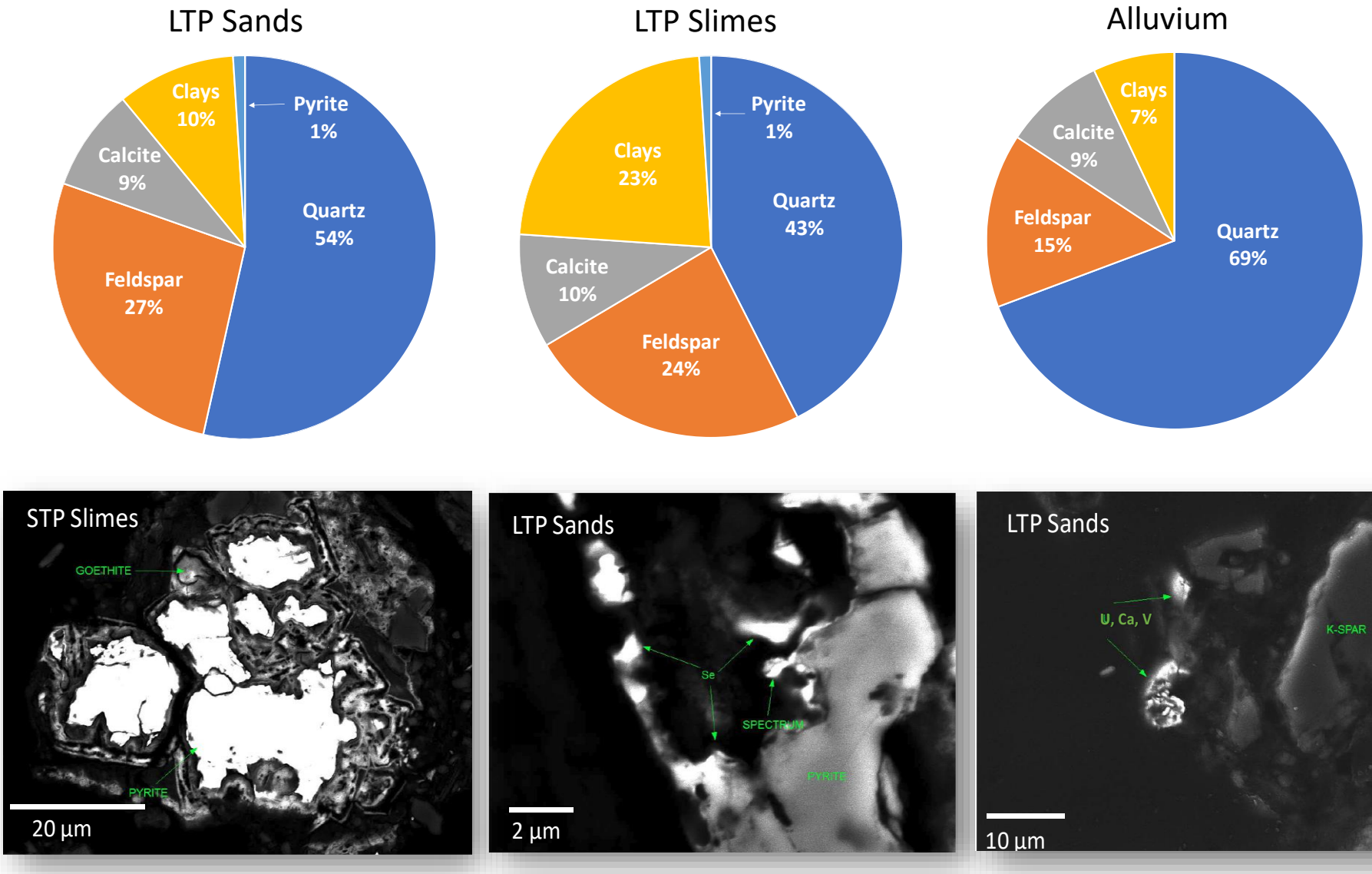

Figure 13: Representative XRD and SEM Mineralogy Results for Tailings and Alluvium.

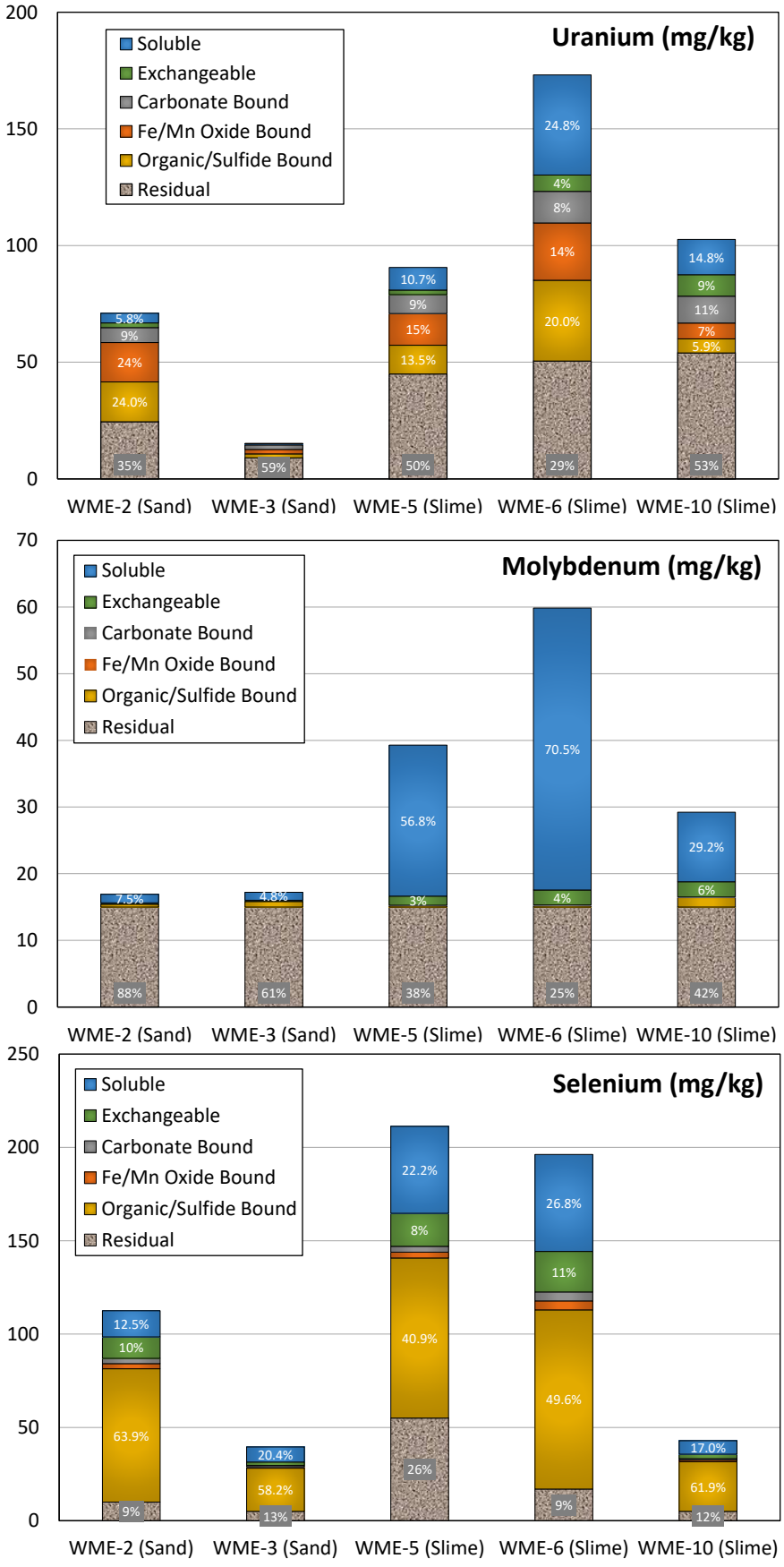

Figure 14: Sequential Selective Extraction Results for U, Mo, and Se in LTP Solids.

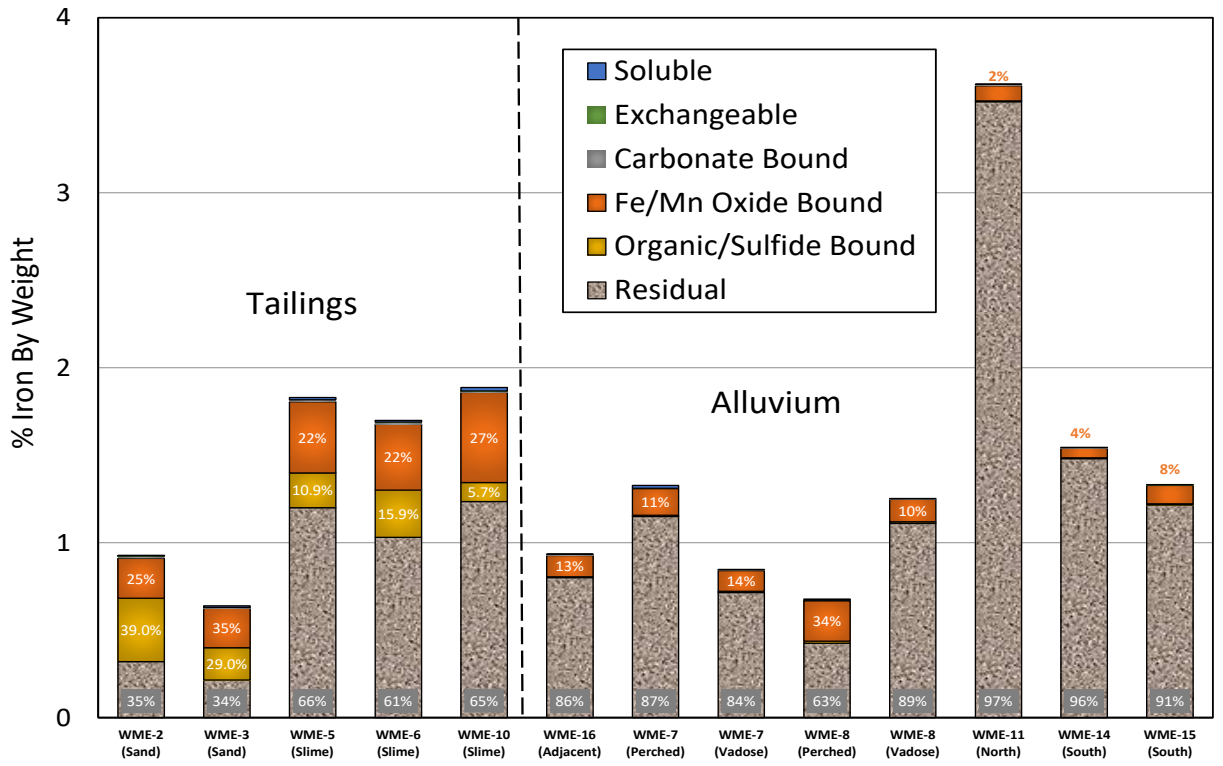

Figure 15: Sequential Selective Extraction Results for Fe in LTP Solids

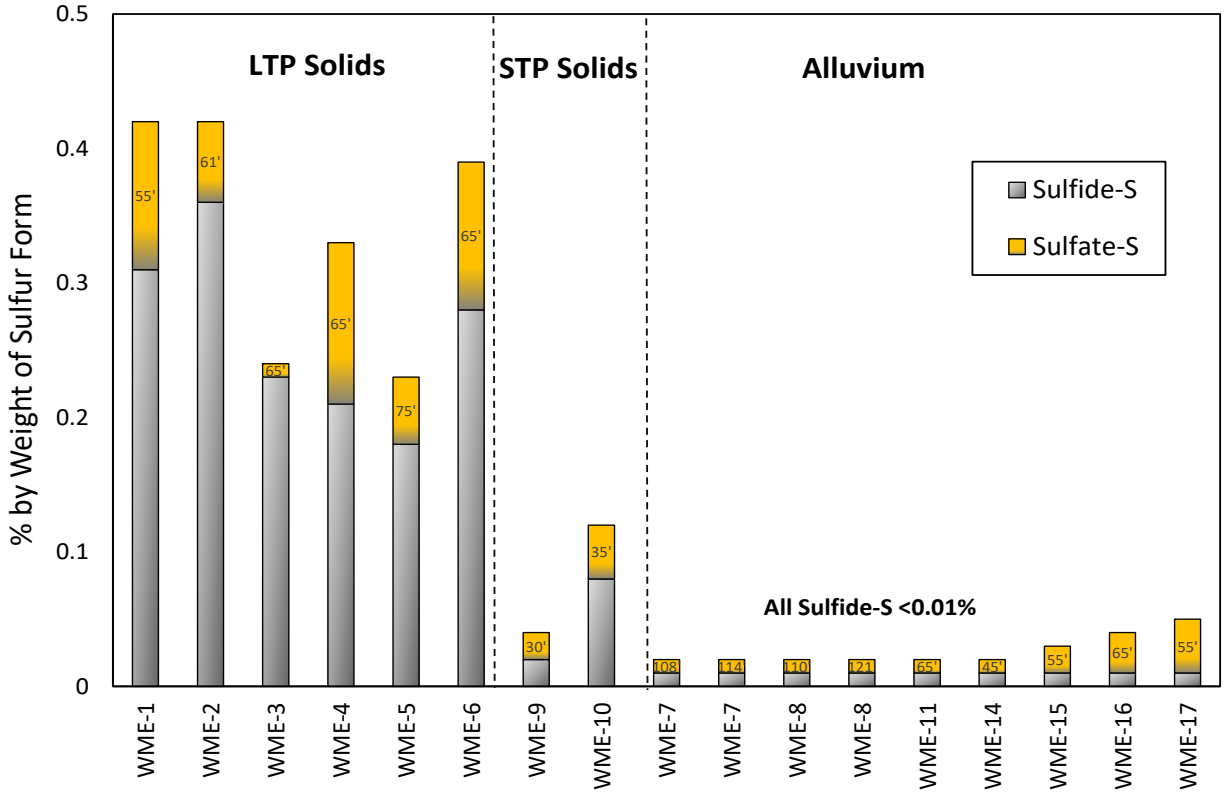

Figure 16: Forms of Sulfur in the Tailings and Alluvium.

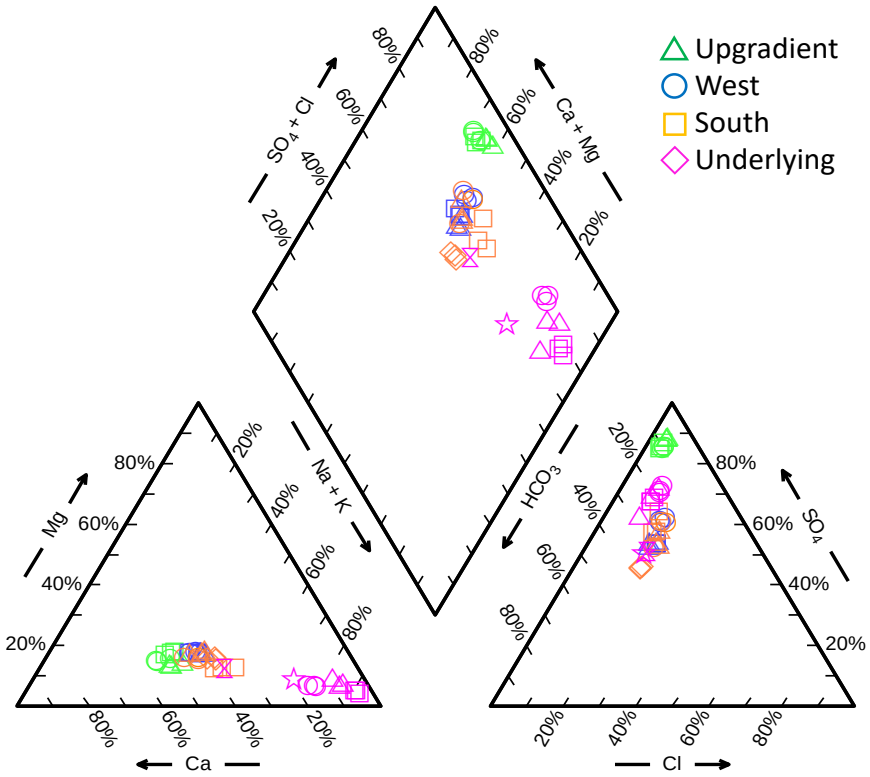

Figure 17: Trilinear Diagram for Alluvial Aquifer Samples Relative to the LTP (2018).

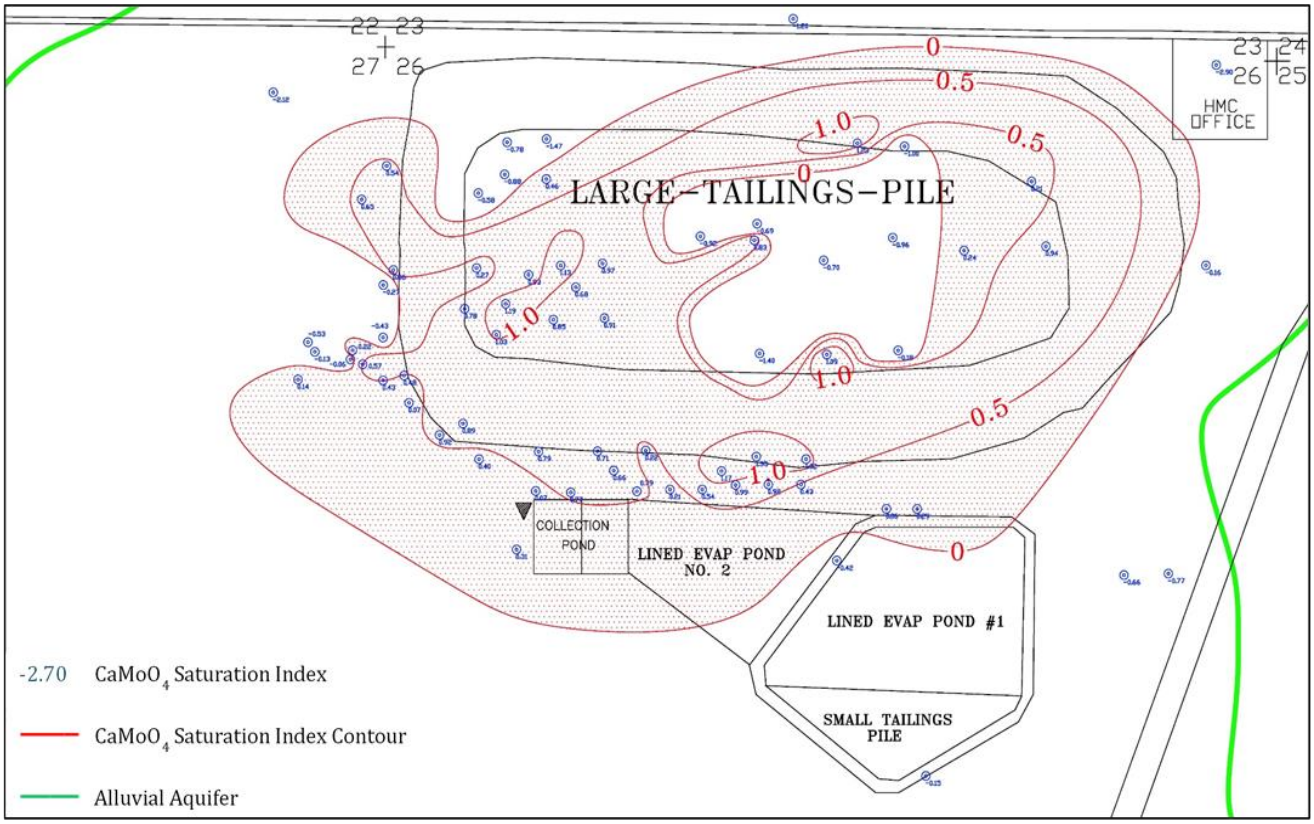

Figure 18: Powellite Saturation Index Values in the Vicinity of the LTP.

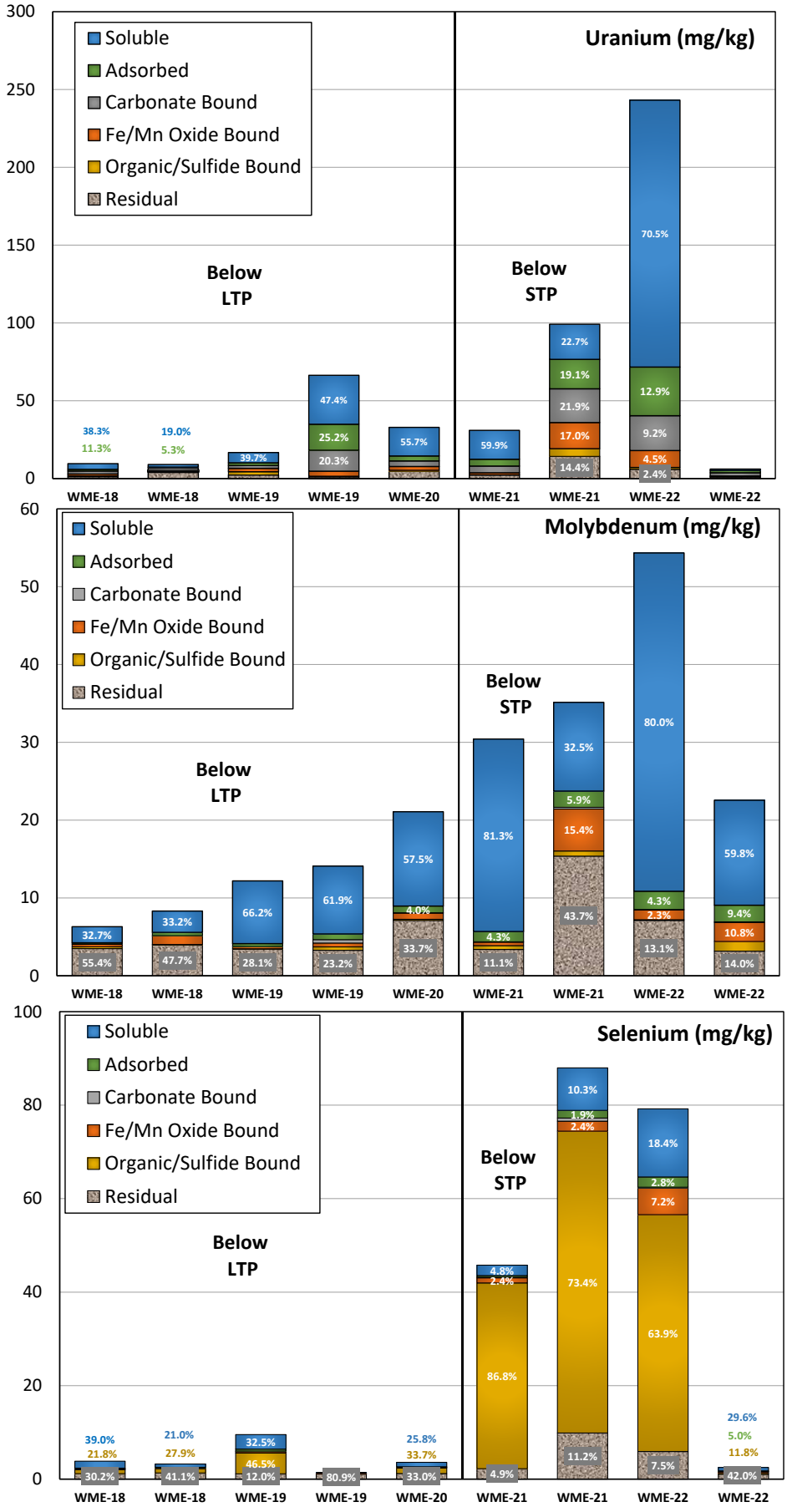

Figure 19: Sequential Selective Extraction Results for U, Mo, and Se in Alluvial Solids.

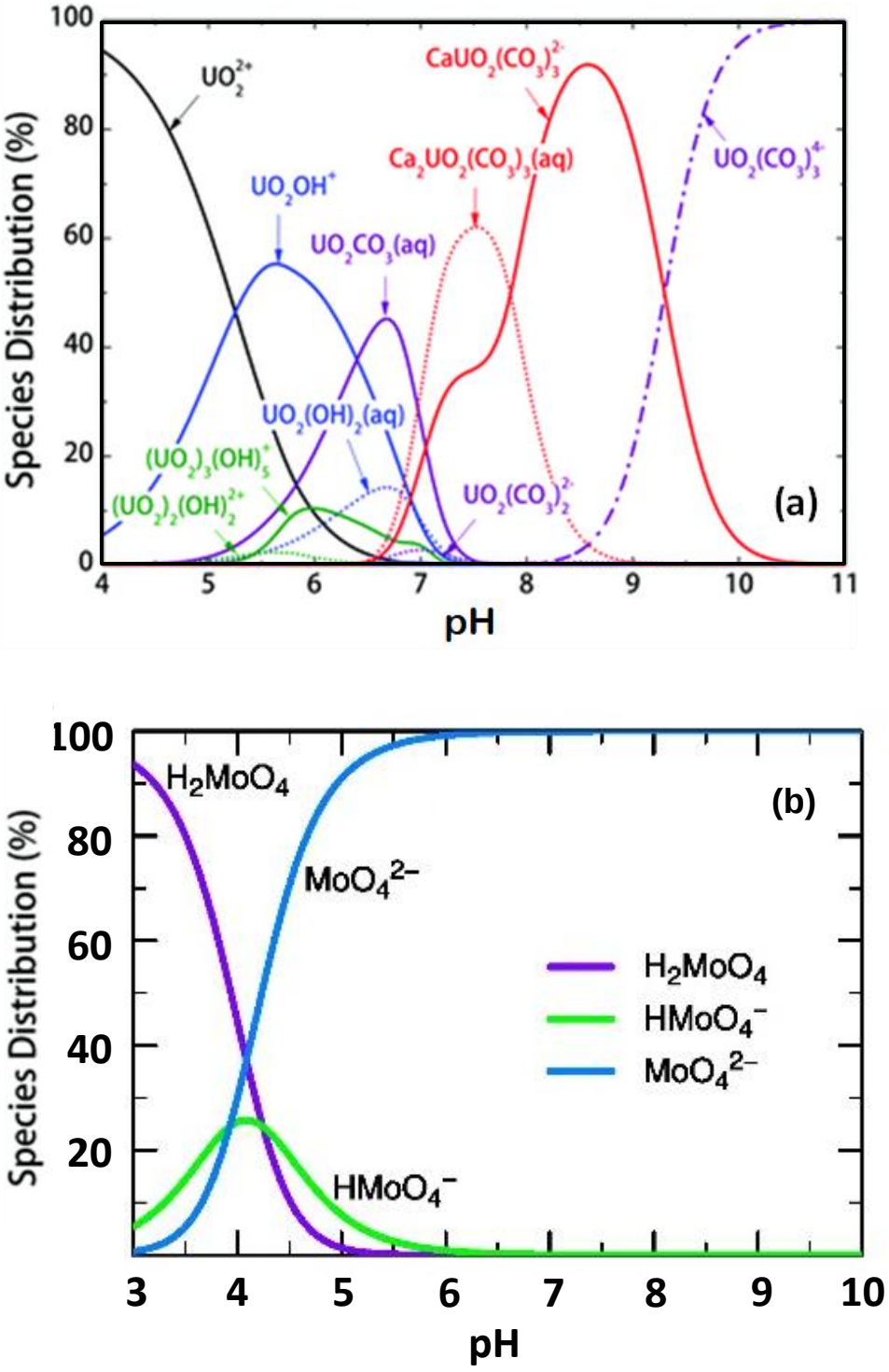

Figure 20: Uranium (a) and Molybdenum (b) Speciation as a Function of pH (Lee and Yun, 2013; Smedley and Kinniburgh, 2017).

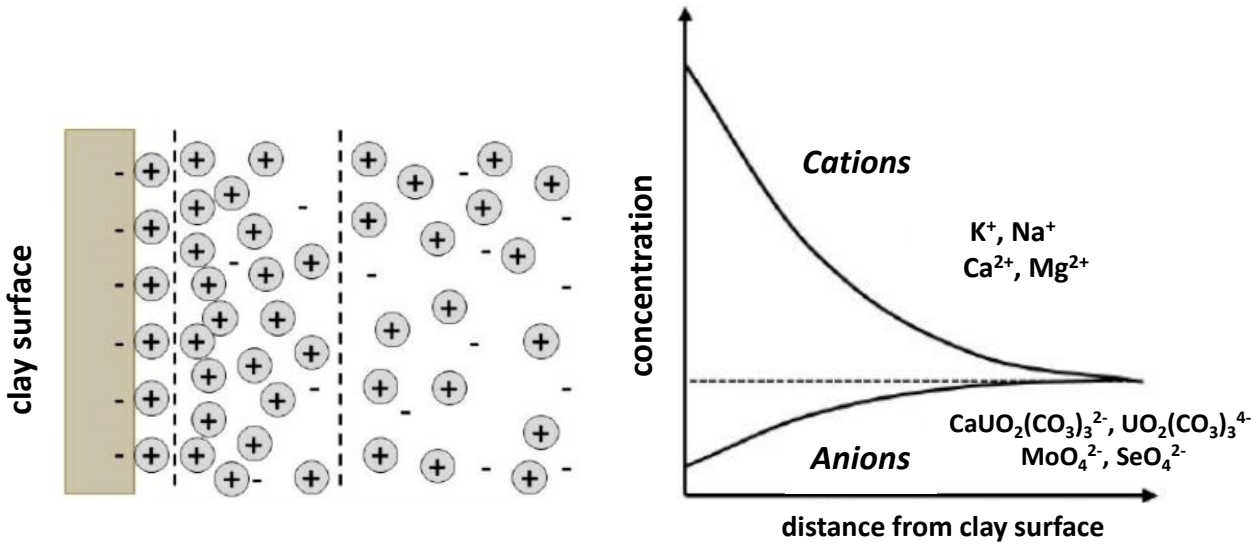

Figure 21: Distribution of Ions Adjacent to a Clay Surface.

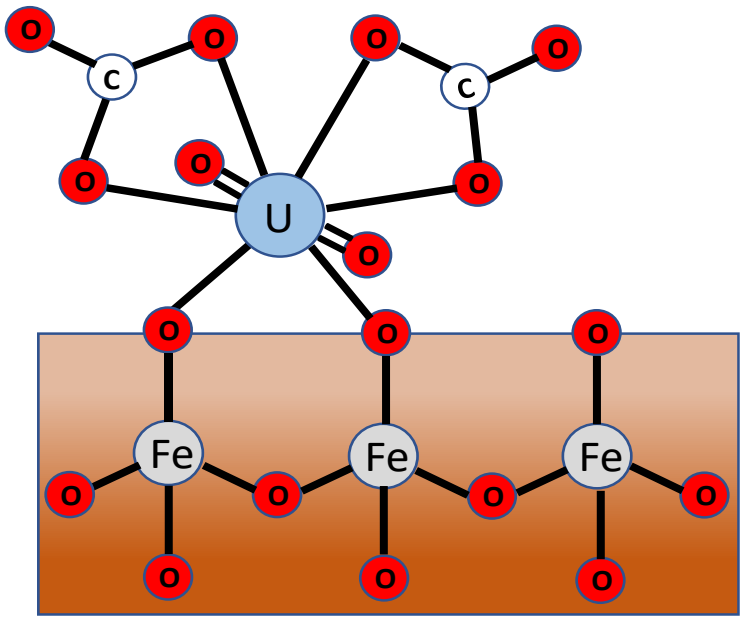

Figure 22: Schematic Representation of U(VI)-Carbonate Complex Adsorption to Ferrihydrite.

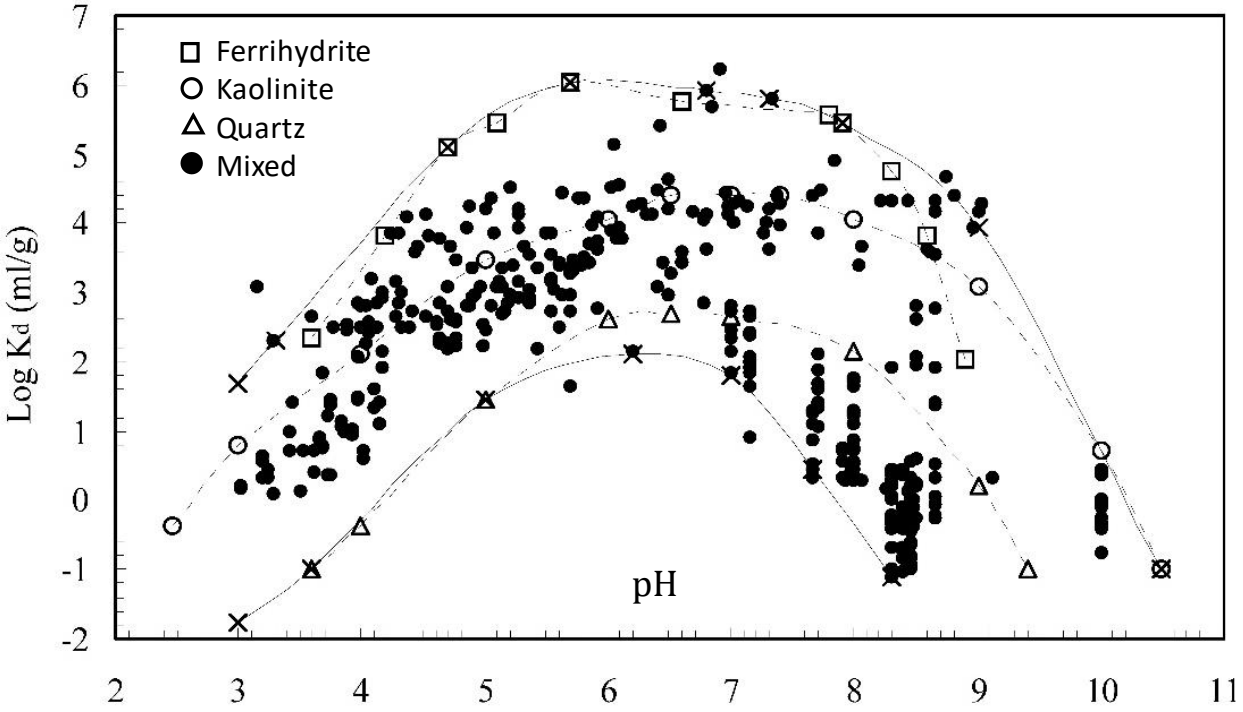

Figure 23: Range of U K_d Values Compiled by the USEPA (1999) for Various Minerals.

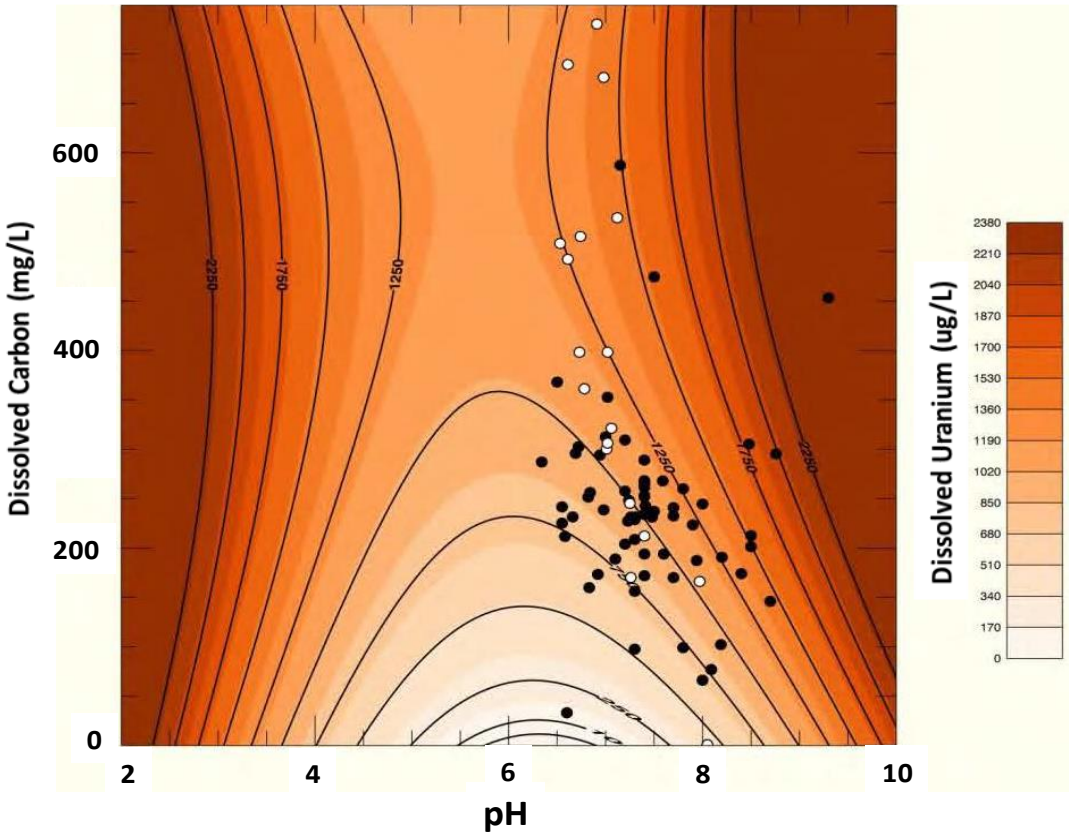

Figure 24: Uranium Concentrations in Equilibrium with Ferrihydrite as a Function of pH and Alkalinity (black and white dots represent background and onsite Bluewater disposal site locations) (DOE, 2014).

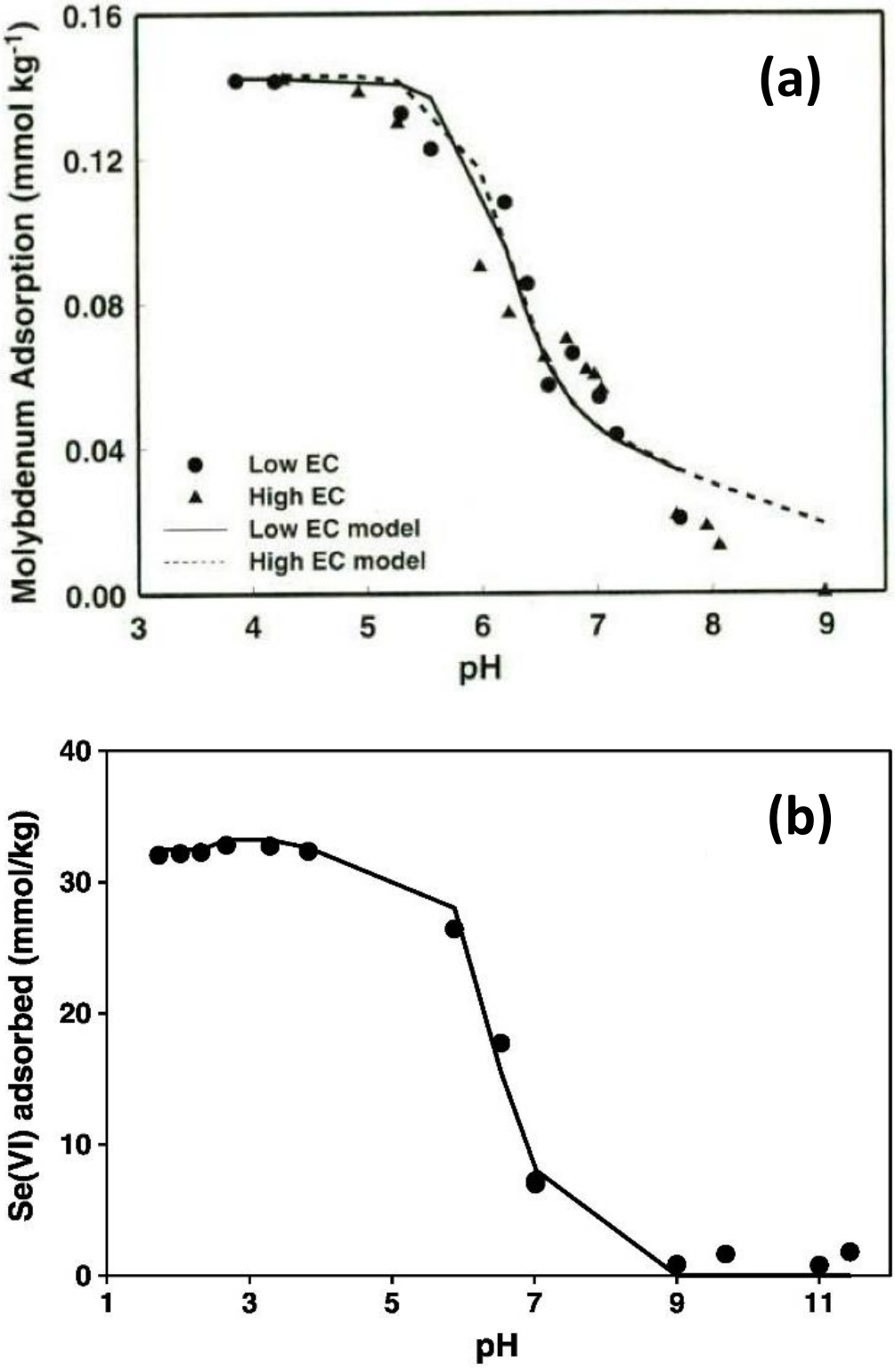

Figure 25: Adsorption Characteristics of (a) Mo on Soil Constituents (Goldberg, 2009) and (b) Se on Ferrihydrite (Goldberg, 2014).

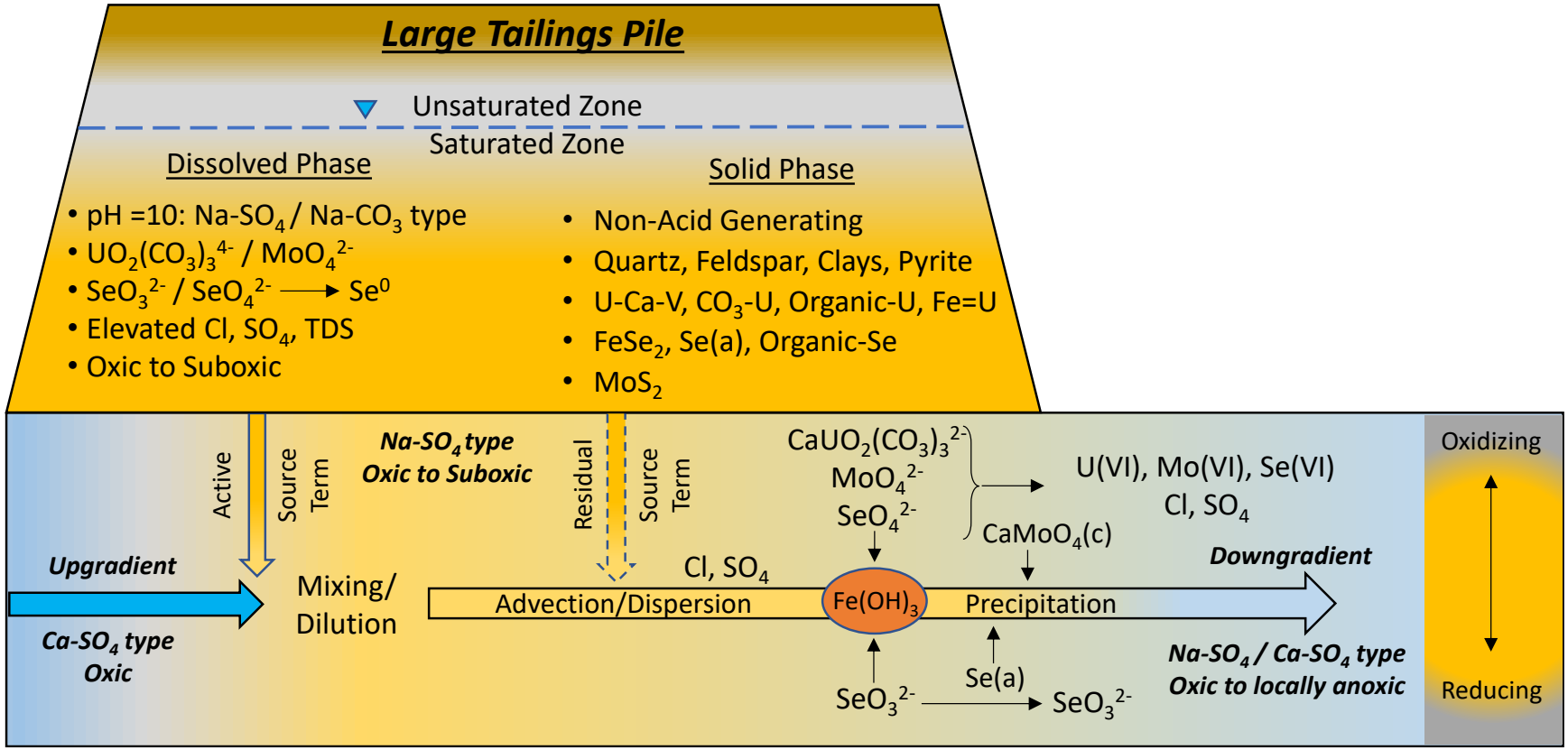

Figure 26: Conceptual Geochemical Model for the LTP and Alluvial Aquifer, Grants Reclamation Project.